THE UNIVERSITY of ADELAIDE

St Kilda Mangrove and Saltmarsh Hypersaline Brine Contamination 2020

Report Prepared for the Department for Environment and Water, by The University of Adelaide. November 2022.

make history.

Citation

Leyden E, Thomas B, and Mosley LM (2022). *St Kilda mangrove and saltmarsh hypersaline brine contamination 2020*. Report Prepared for the Department for Environment and Water, by The University of Adelaide. November 2022.

THE UNIVERSITY of ADELAIDE

www.adelaide.edu.au

Disclaimer

This report has been prepared by The University of Adelaide and contains independent scientific/technical advice to inform government decision-making. The independent findings and recommendations of this report are subject to separate and further consideration and decision-making processes and do not necessarily represent the views of the South Australian Government or Department for Environment and Water.

Table of Contents

Executive Summary

In 2020, the South Australian Government became aware of the death of saltmarsh and mangrove vegetation near St Kilda, adjacent Section 2 of the Dry Creek Salt Fields. The University of Adelaide has undertaken a project to develop a conceptual model of the area to summarise relevant scientific knowledge of the hydrology and ecology of the site, determine likely environmental impact pathways, identify knowledge gaps and provide potential future management options for the local area for the Department for Environment and Water (DEW) to consider.

Relevant experts and stakeholders were consulted and available scientific data collated and summarised. Two conceptual site models were developed and a summary of conditions and events over time are reported here. Knowledge gaps and limitations have been identified and potential strategies for future work are outlined.

Key Findings:

- The increase in the surface water level in Section 2 ponds of the saltfield from December 2019 to October 2020, due to discharge from Section 3, increased the recharge to the groundwater mound under the ponds. Surface cracking of the gypsum crust in the ponds further enhanced transport of surface water to the groundwater mound. The elevated groundwater mound under the ponds in Section 2 increased the hydraulic gradient towards the intertidal zone.
- Upon refill, the pond surface water became extremely hypersaline due to a combination of highly saline input water and dissolution of surface salts from the surface of Section 2 ponds.
- Due to hydraulic connectivity with the pond surface water, the groundwater underneath the ponds also became extremely hypersaline. This groundwater moved towards the intertidal zone under the increased hydraulic gradient.
- There are numerous hydraulic pathways of groundwater flow from the ponds to the intertidal zone, including remnant creek lines and transmissive sediments under the bund wall.
- As sediments became hypersaline and waterlogged in the intertidal zone, vegetation (saltmarsh, mangrove) death occurred rapidly. This was observed from mid to late 2020.
- Spatial satellite analysis determined retrospectively that 24 hectares of vegetation death was recorded in the intertidal zone adjacent Section 2, including 9 hectares of mangrove, 10 hectares of saltmarsh, and nearly 5 hectares of bare, sparsely vegetated, and aquatic ecosystems. It is likely there is a greater area which recorded vegetation stress following impact between the recorded dead vegetation zone and the healthy vegetation zone.
- It is probable that other ecosystem impacts occurred, like stress or acute toxicity to benthic invertebrates and fish communities, as well as changes in sediment/soil physical characteristics, however, there is currently no available ecosystem data to quantitatively assess these impacts.
- Once the surface water level reduced in Section 2, the recharge to the groundwater mound underneath the ponds in Section 2 decreased and the hydraulic gradient to the adjacent intertidal zone reduced. Less hypersaline groundwater was moving towards the intertidal area and tidal flushing diluted surficial sediment salinity in the intertidal zone.
- Sediments and tidal flushing are highly heterogenous and spatially variable across the intertidal zone of the affected area. Barriers (bunds, chenier ridges, sea wrack) to tidal flushing limit some sediments from benefiting from dilution by tidal water. This also reduce the ability of vegetation in these areas to recover from hypersalinity impact.

- Fine grained sediments (muds/clays), sediments in low elevation areas, deeper sediments and those close to the Section 2 bund remain higher in salinity than higher elevation, surface and coarser sediments further away from the Section 2 bund, some of which have returned to pre-impact salinity.
- Hypersaline water has been flushed from some surficial sediments, however, there is no recent data on the salinity of deeper sediments.
- Seedling emergence and regeneration has been observed in some limited areas (high saltmarsh), and propagules have been observed in the mangrove area since spring 2021, but the lack of recent vegetation survey data makes the quantitative analysis of vegetation recovery trends impossible. It is also unclear whether saltmarsh and mangrove species can survive once roots extend into deeper sediment layers (due to residual hypersalinity in the subsurface sediments).
- While there was sufficient information to develop a broad-scale conceptual model there were some knowledge gaps relating to spatial and temporal resolution of data and site characteristics

Recommendations:

The conceptual model indicates that the impact to the intertidal zone, including death of saltmarsh and mangrove vegetation, was a result of leakage of extremely hypersaline water when the pond level in Section 2 was refilled from late 2019. It is recommended that the water level of Section 2 ponds is kept low while extreme pond surface hypersalinity remains, to minimise the hydraulic head difference between the pond and the intertidal zone. This will limit the movement of salt from the pond to the intertidal zone and to allow tidal flushing to dilute residual hypersalinity in the sediment of the intertidal zone adjacent the Section 2 bund following impact.

Future work should consider increasing the spatial and temporal data set to track recovery trajectories of the site, expand data on soil/sediment type and salt accumulation in the intertidal zone, assess aquifer boundaries within the pond and under the bund, and better understand the bund wall permeability, particularly in regard to hydraulic pathways such as remnant creek lines and scour areas. A monitoring program should be designed and implemented at the site to better assess and quantify the ongoing impact of the salt pond on the intertidal zone and ecosystem recovery trajectories.

Increased tidal flushing pathways and/or reinstating seepage channels along the bund wall to reduce water logging could also be considered but would require engineering design and construction work, and risk management. A better understanding of tidal water movement across the intertidal zone would aid in assessing where vegetation recovery is likely and where it may continue to be affected.

Long term, efforts to assess the removal of the hypersaline pollution pathway (i.e. tidal restoration of Section 2 and 3) could also be considered, especially in the context of climate change and sea level rise.

St Kilda mangrove and saltmarsh hypersaline brine contamination 2020 conceptual model

Intertidal Zone Adjacent Section 2

1 Hypersaline brine from Section 3 ponds caused salt input and high groundwater levels in Section 2 ponds.

2 Groundwater flows push hypersaline brine through cracked gypsum crust and transmissive aquifers into impacted area.

3 Geology and topography of the site creates barriers and pathways to tidal flushing of hypersaline brine from impacted area.

4 Exposure to high salinity waters and waterlogged soils caused the death of saltmarsh and mangrove vegetation.

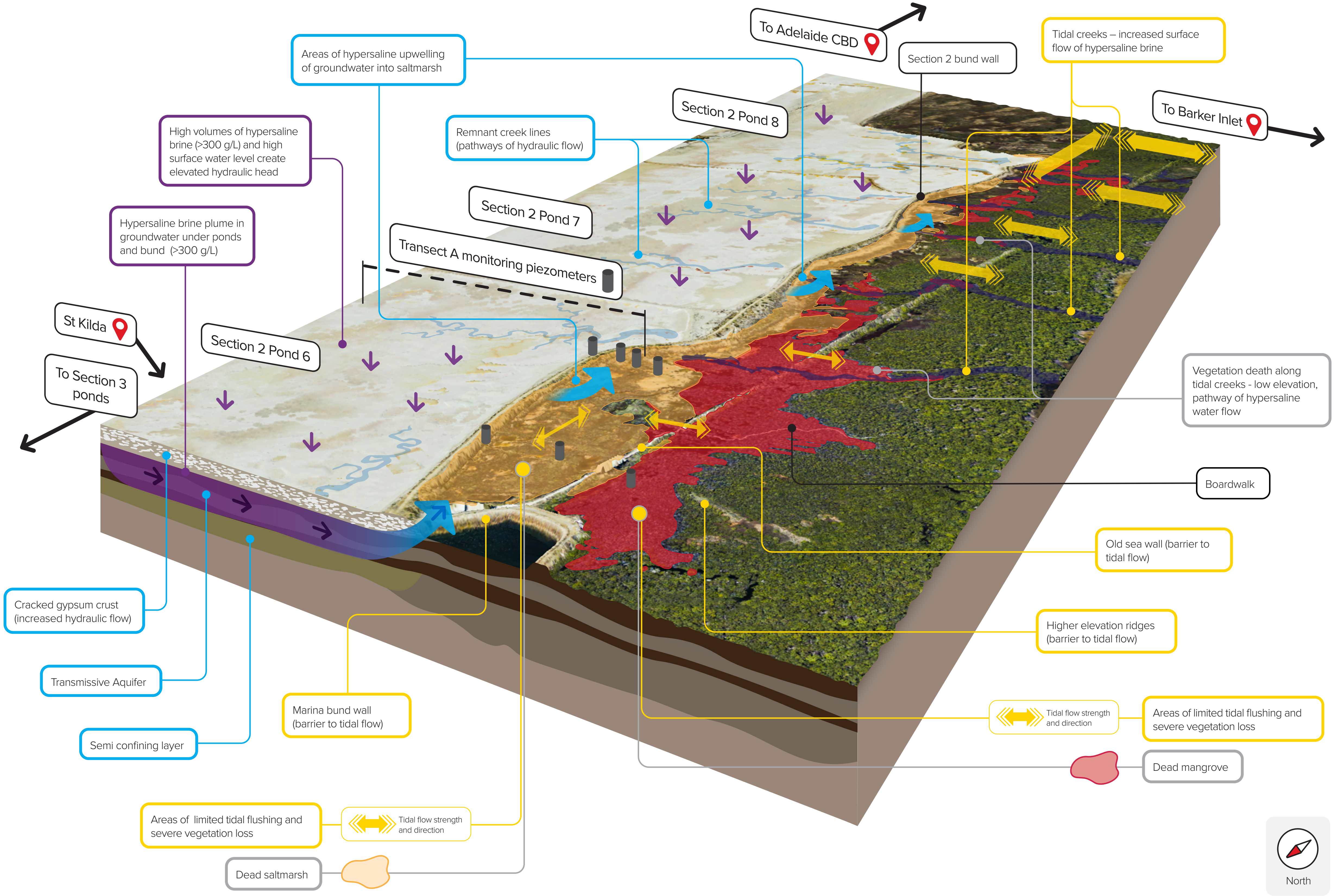

Published Nov 2022

Government of South Australia
THE UNIVERSITY of ADELAIDE

DRY CREEK TIMELINE

Operational Phase Pre-2013

Level in pond high, medium hypersalinity

Slow leakage to intertidal zone under bunds

Salt scalds apparent in interrtidal zone

Drying Phase 2014

Level in pond reduces, and hydraulic gradient to intertidal zone reduces

Zone of mixing with tidal waters under bund established

Drying causes chemistry changes in gypsum crust

Holding Pattern summer evaporation, winter ponding 2014-2019

Drying = chemical changes to gypsum crust

Rain pools on surface in winter, then evaporate in summer

Surface salts dissolve. Pond surface water and groundwater become extremely hypersaline

Refilling Phase December 2019 - October 2020

Refilling with hypersaline water, large hydraulic gradient towards intertidal zone through Aquifer B and bund

Sideways flow of extremely hypersaline brine through groundwater to intertidal zone

Hypersaline sediments in intertidal zone observed, vegatation death occurs

Pond pumping, summer evaporation and winter ponding 2021-2022

Tidal flushing reduces salinity in some coarse sediments and higher elevation sediments

Areas of highly saline porewaters in fine sediments, in sediments in lower elevations, deeper layers and in areas where tidal constriction present

Vegetation slow to recover

OPERATION PHASE 1950-2013

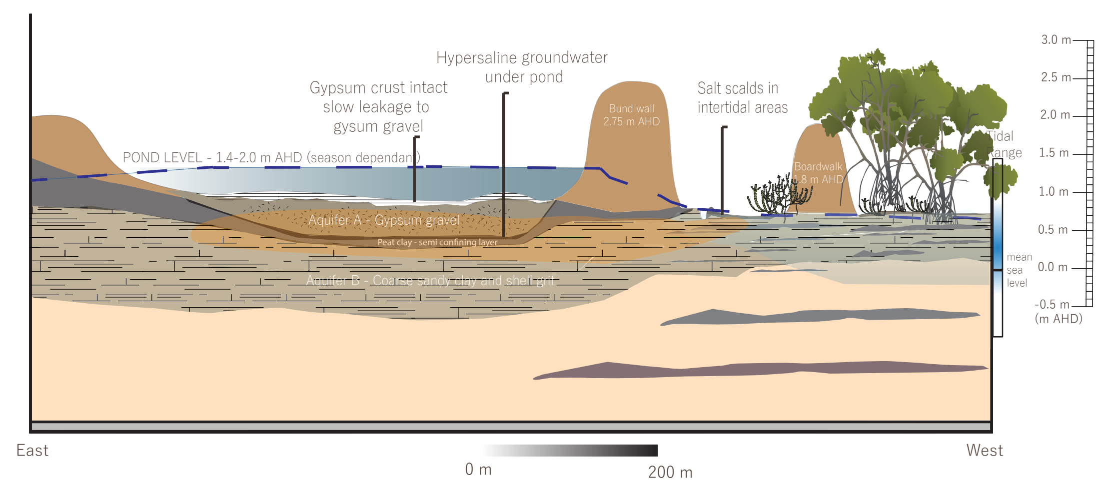

DRYING PHASE - 2014

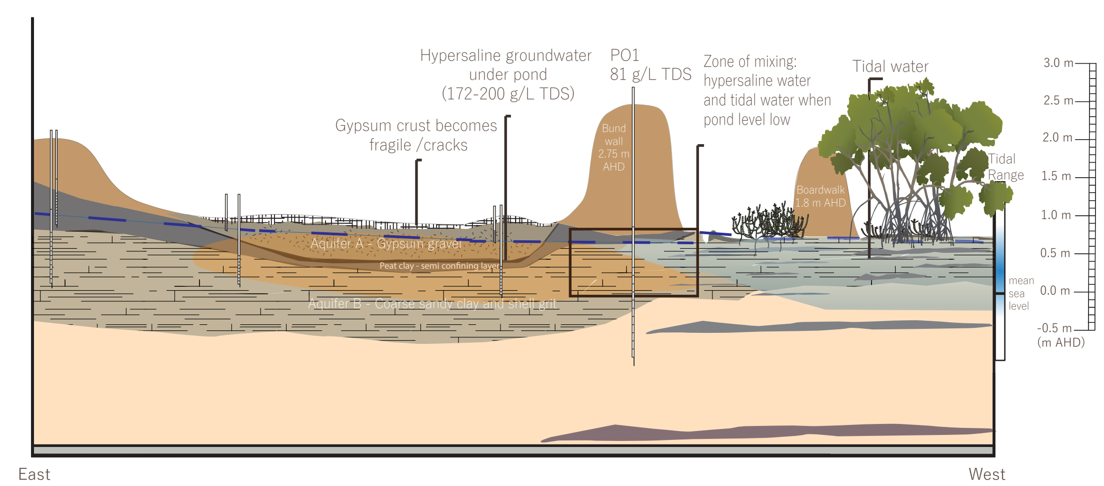

HOLDING PATTERN - 2014-2019

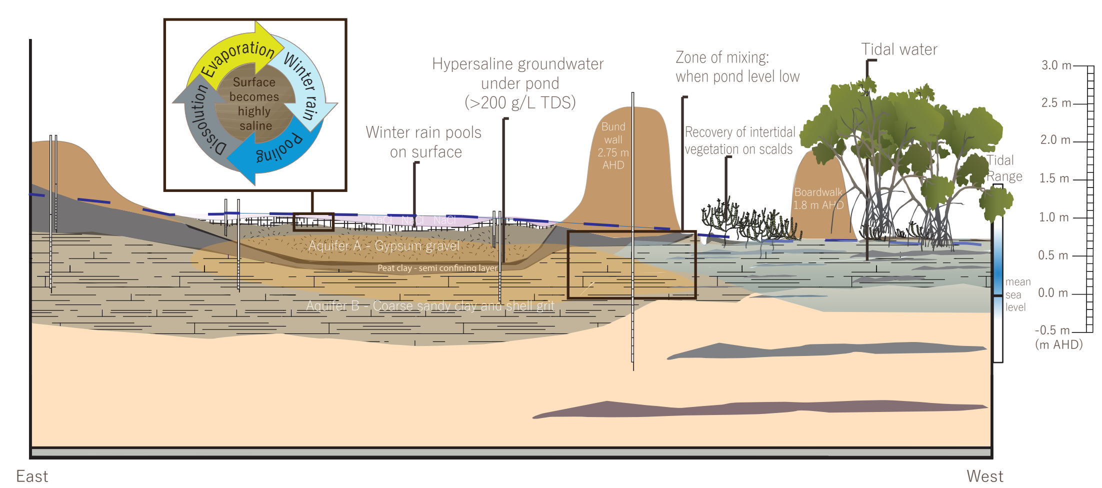

REFILLING PHASE Dec 2019 - Oct 2020

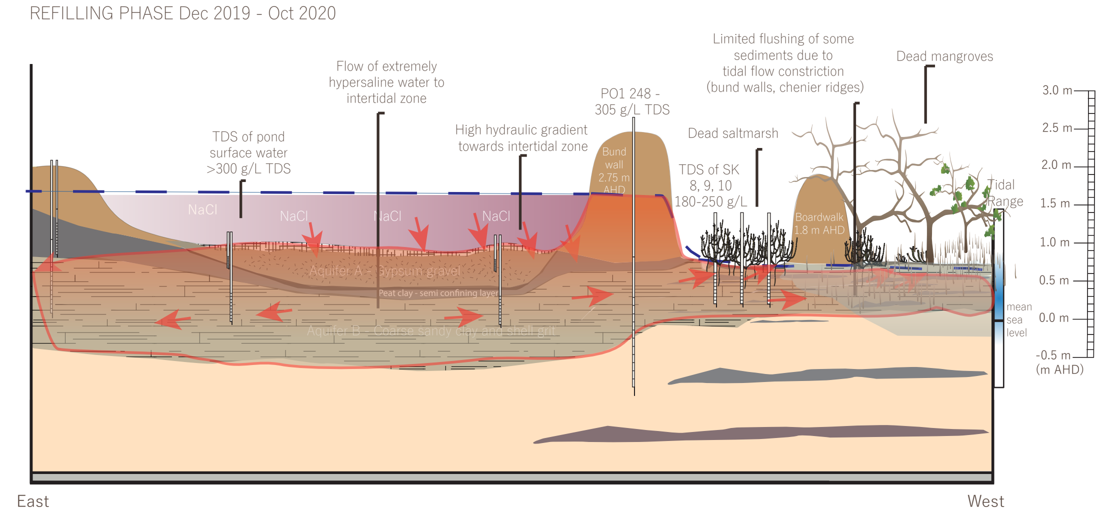

DRAINING, DRYING, WINTER PONDING : 2021 - 2022

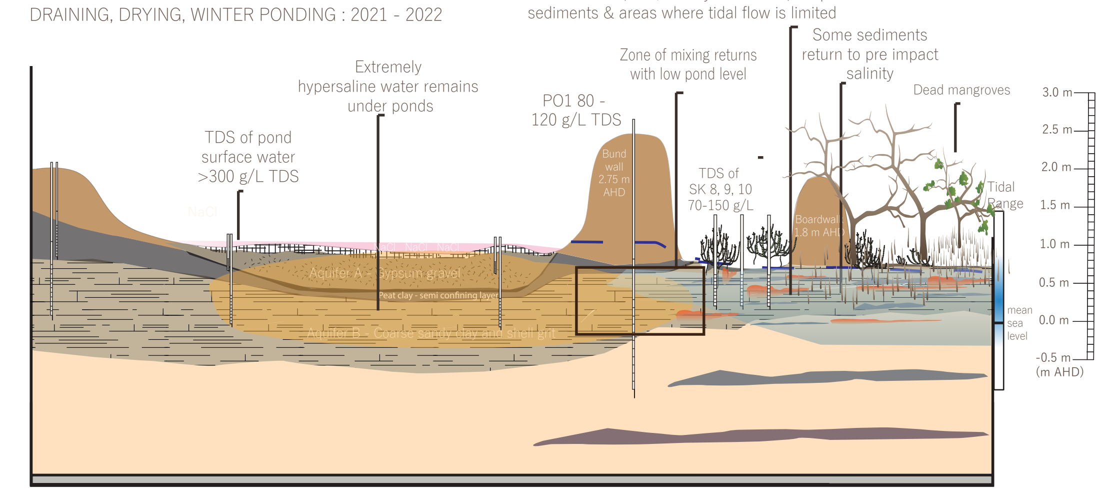

Operation Phase: Section 2 and adjacent intertidal zone: Aerial Photographs from 1997 data set

Drying Phase/Holding Pattern: Section 2 Ponds and adjacent intertidal zone

Refilling/Post impact: Section 2 Ponds and adjacent intertidal zone Area of vegetation dieback represented by orange crosshatch

1. Introduction

1.1. Background

The Dry Creek salt fields (4,000 ha) are located along the coast, 12 km NW of Adelaide, South Australia. The ponds extend about 35 km from Dry Creek (Section 1) to St Kilda (Section 2) to Port Gawler (Section 3) to Middle Beach (Section 4). Salt was produced at the site from the late 1930's by evaporating seawater pumped into a series of concentrating ponds to the point where common salt (NaCl or halite) precipitates. The less soluble salts, iron oxide (e.g. $Fe(OH)_3$) and calcite ($CaCO_3$), followed by gypsum ($CaSO_4.2H_2O$), were precipitated out during passage and evaporation of seawater along the chain of ponds. Salt production operation ceased in 2013. Since this time, a temporary 'holding pattern' was established at the site. The holding pattern allows seawater to be pumped into the northern section (Sections 4 and 3) with the intention of maintaining the salinity gradient and pond habitat for invertebrates and wading shorebirds. Currently brine exits Section 3 (from pond PA 5) and is pumped into the Bolivar channel where it is diluted with discharges from the SA Water waste treatment plant (to a target salinity of 45 g/L Total Dissolved Salts (TDS) – set by the South Australia Environment Protection Authority). The diluted water returns to Gulf St. Vincent. During the holding pattern, the ponds in Section 3 both increased in salinity and depth. Data suggests salinities were highly variable compared to that recorded during salt production operation phases (EPA data). This was due to more variable movement and control of salt through the system, compared to the salt production operation phase.

The southern sections (Sections 2 and 1) were drained and dried from late 2013 onward. Various infilling activities have occurred in Section 1, while Section 2 has remained mostly dry between 2014 and 2019, except for pooling on the ponds following winter rainfall, and a wastewater trial by SA Water in some Section 2 ponds (2014-2018). During the time when the pond level was dry or very low, intertidal vegetation began to recolonise (evidenced from aerial images) in previously salt scalded areas directly west of the bund wall. The drying of the ponds, and subsequent pooling of winter rainfall followed by evaporation in summer between 2014-2019, altered the surface minerology and chemistry of the pond surface in Section 2, with the surface becoming dominant in both gypsum ($CaSO_4$) and halite (NaCl). Cracking was also observed in the gypsum crust during this time. A part of Section 2 (PA 8, 9 and 10) was used for a wastewater trial in between 2015 and 2018. A low surface water level and low salinity was maintained during this trial and little evidence for impact of vegetation in the intertidal zone was observed during this time (from aerial images).

Over time, the availability of water from the SA Water waste treatment plant has declined, as water diversions to the Northern Irrigation Scheme increased. Consequently, there has been less wastewater available to dilute the brine from PA 5 in the Bolivar Channel and lower volumes of brine has been able to be discharged. In late 2019 and during 2020, to prevent build-up of water in Section 3, the brine was instead discharged in the ponds of Section 2 and then moved south to Section 1. The pond level in Section 2 (PA 6,7, 8, 9 and 10) increased substantially during this time, to the highest level since the drying of the ponds when salt production ceased.

In September 2020, over 24 hectares of vegetation death in the intertidal zone adjacent Section 2 was observed, including 9 hectares of mangrove, 10 hectares of saltmarsh, and nearly 5 hectares of bare, sparsely vegetated, or aquatic ecosystems DEW (2021). A larger area of vegetation stress was identified by (Dittmann et al. 2022). Extremely hypersaline water (> 100-200 g/L TDS, 8 x seawater) was observed in surface water, monitoring piezometers along the bund wall and intertidal zone, and extremely hypersaline sediments were recorded in transects affected by vegetation death.

1.2. Project aims

The project aims to bring together scientific and other information from a range of stakeholders which have been responding to the impact at the site. Relevant stakeholders (Table 1) were consulted via online and in person meetings, and information was collated in brief in this document. From the information received, conceptual site models have been developed for consultation.

Table 1: List of stakeholders consulted in this project

Stakeholder	Department	Contact
South Australian Government	Department for Environment and Water (DEW)	Matthew Miles Dr. Dan Rogers
	State Herbarium	Doug Fotheringham
	Department for Energy and Mining (DEM)	Gabor Bekesi
	South Australian Environment Protection Authority	David Palmer Peter Goonan
Delta Environment Consulting		Peri Coleman
EcoProTem Consulting		Faith Coleman
The University of Adelaide	School of Biological Sciences	Dr. Alice Jones
The University of Adelaide	School of Agriculture, Food and Wine	Dr. Brett Thomas A/Prof. Luke Mosley
Flinders University	College of Science and Engineering	Prof. Sabine Dittmann

2. The Dry Creek Salt Ponds

2.1. Reference comparisons for salinity

The units used to measure salinity change depending on application and reporting procedures. For simplification, units are referred to in Total Dissolved Solids (TDS) in grams/Litre (g/L) in this report. Where other units are reported in information received from other sources, the units have been converted as outlined in Lionberger et al. (2004).

Salinities are listed (Table 2) for simple reference, approximation and comparison purposes.

Table 2 Selected reference salinities for comparison and units used in this report, conversions from (Lionberger et al. 2004)

	TDS (mg/L)	TDS (g/L)	Practical salinity unit (psu)	Parts per thousand[1]	Approx. EC (mS/cm or dS/m)[2]	Specific Gravity
Gulf of St Vincent Seawater (approx.)	38 000	38	37	35	~40-50	1.026
Hypersaline brine in pond surface water in Section 2 pre closure (approx. values)	199 000	199	199	199	Above 150	1.15
Hypersaline brine in pond surface water in Section 2 after refilling (approx. values)	362 000	362	292	353	n/a	1.23
P 01 piezometer 2014	216 587	267	227	260	~158	1.173
P 01 piezometer (21/12/2020)	312 000	312	258.9	304	n/a	1.20

[1] TDS (g/L) is expressed as parts per thousand (ppt) by dividing by 1.026. This assumes an average seawater density of 1.026 g/ml based on a salinity of 37 psu and a water temperature of 20 C. Given densities are variable due to hypersalinity and temperatures are sometime unavailable ppt is avoided in this report and put in the table purely for approximation purposes

[2] EC of a solution will vary depending on the concentrations and activity of ions in the solution and temperature – therefore EC is given purely for approximation purposes

2.2. Location of Dry Creek Salt Ponds

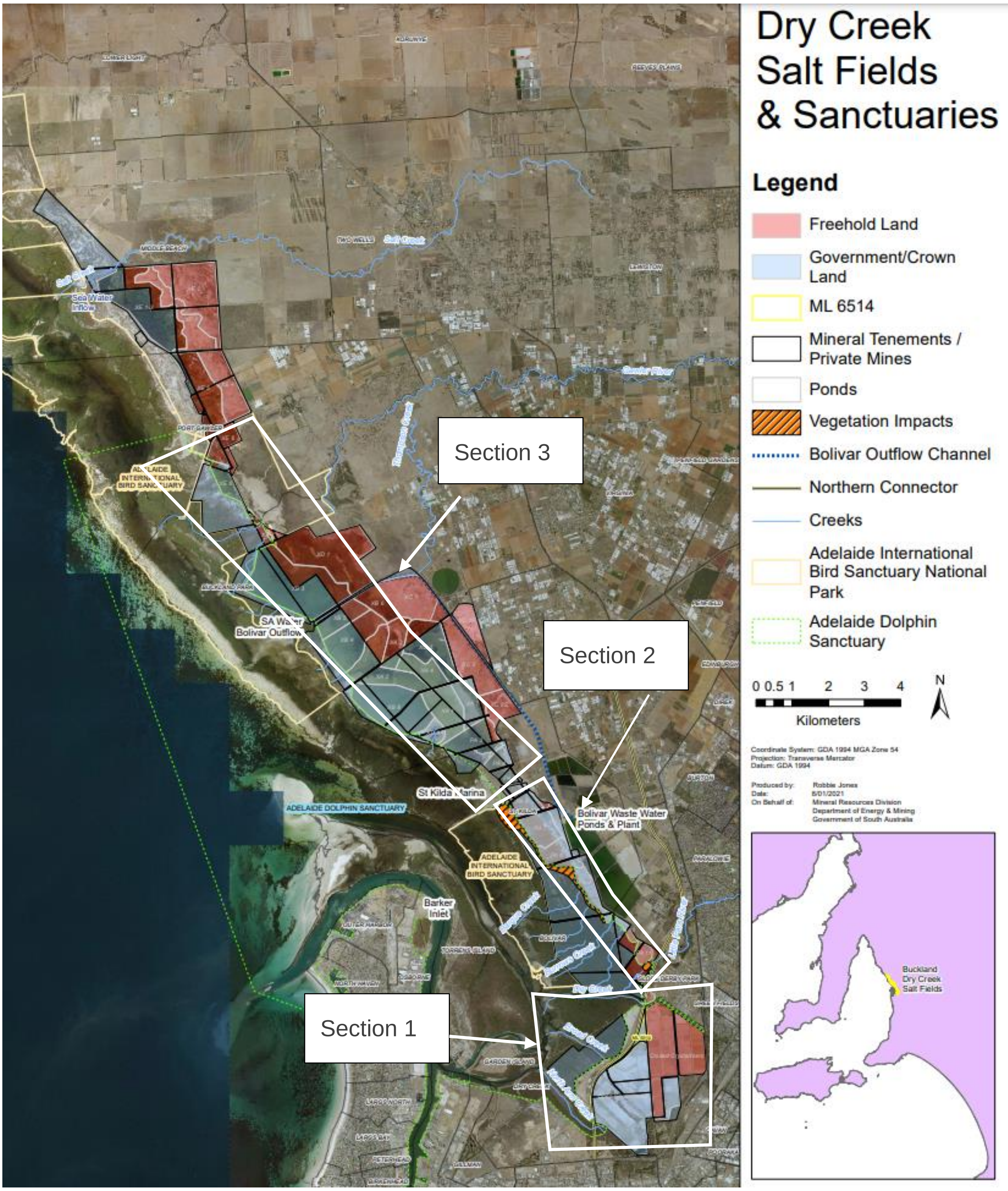

Figure 1 Location of the Dry Creek Salt Fields and overview of land ownership (Source: DEM)

2.3. Regional Site Geology and Hydrogeology

Section 2 (**Error! Reference source not found.**) is characterised by low lying land underlain by marine and estuarine soils with shallow, saline groundwater. The site has been altered by drainage, filling and construction of bunds to form salt evaporation ponds. The land surface slopes gradually from approximately 2.5 m AHD in the eastern portion of the site to 0.8 m AHD on the western side Tonkin (2015).

The eastern (landward) portion of the Section 2 lies in the Lower Alluvial Plain geomorphic unit. This unit is characterised by alluvial soils and outwash fan deposits and is named the Pooraka Formation (Pleistocene age). The presence of sandy or gravel lenses (representing former, now buried drainage lines) are common in the Pooraka Formation and generally have less saline (brackish) groundwater than the marine sediments (Tonkin 2015).

The western portion of the ponds and adjacent intertidal zone is represented by the St Kilda Formation which formed during the last 10 000 years. The St Kilda Formation consists of marine sediments deposited under beach foreshore, coastal dune, estuarine and back barrier lagoonal environments (sedimentary facies) and ranges in thickness from 1 m in the east to 6 meters in the west. The unconsolidated St Kilda Formation sediments are highly variable and contain inter bedded silts, clays, sands and (samphire and mangrove) muds with varying contents of organic matter and shells. Shallow, saline groundwater associated with the St Kilda Formation often presents a sulphurous odour and soils are sulfidic (i.e. contain acid sulfate potential) (Tonkin 2015, Fitzpatrick et al. 2014, Thomas 2010)

The St Kilda Formation is underlain by the Glanville Formation and Hindmarsh Clay (Pleistocene age) ((Belperio et al. 1995). The marine Glanville Formation consists of grey shelly sands to sandy marl and clays. Groundwater present in the Glanville Formation is only partially confined and has a similar phreatic surface to the groundwater system in the overlying St Kilda Formation. The Hindmarsh Clay forms an aquitard (approximately 70 m thick) at the base of this sequence and separates the Quaternary and underlying Tertiary aquifers (Tonkin 2015).

Information and data from intertidal zone west of Section 2 is collated in detail in Thomas (2010) and summarised here. The intertidal area westward of Section 2 is low lying land with elevation ranging from -1.0 m AHD on the tidal mudflats to 1.5 m AHD on the intertidal chenier ridges (remnant dune systems). Networks of tidal creeks run in an east to west direction through the saltmarsh and mangrove areas. These creeks adjoin remnant creek channels in the Section 2 ponds. The vegetation type and species in the intertidal zone is directly related to the topography and consequent degree of tidal inundation (Thomas 2010). Table 3 below is a general guide to which vegetation type may inhabit different elevations in intertidal zone adjacent Section 2. However, it must be noted that some species within these vegetation types are able to withstand waterlogged soils, whereas others tolerate only occasional inundation (Fotheringham et al. 2019, Coleman et al. 2017). Species distribution within vegetation types will change over small elevation distances (centimetres) due to the degree of inundation.

Table 3 General guide to elevation and vegetation type in the intertidal zone (Thomas 2010)

Elevation	Vegetation Type
-1.0 to 0.0 m AHD	Seagrass and mudflats
0.0 to 1.0 m AHD	Mangrove trees
1.0 to 1.5 m AHD	Saltmarsh vegetation

The bund walls of the saltfield, which run north/north-west to south, are the highest land features in the area, between 1.5 and 2.75 m AHD high. The old bund wall (the current St Kilda Mangrove boardwalk – hereafter 'boardwalk bund') is lower at 1.5 m to 2.0 m AHD high. It was built in the 1890s by scouring sediment from either side of the levee to form the embankment. There are several breached sections along its length which allow tidal flushing through creek lines into the intertidal area east of the boardwalk bund. The boardwalk bund joins a 3 m AHD high embankment that runs east-west beside the St Kilda marina channel. The new bund wall ('Section 2 bund') separating Section 2 and the intertidal zone runs is 2.75 m AHD high and runs parallel to the boardwalk bund (Thomas 2010). Further detail on this bund is outlined in section 2.5 below.

2.4. Pond scale hydrogeology in Section 2

Piezometers were installed in the ponds of Section 2, and the east and west bund walls, by Tonkin Consulting (Tonkin 2015). At the same time surveys were completed by CSIRO (Fitzpatrick et al. 2014), that allowed the assessment of the shallow aquifers underlying the pond (present within the St Kilda Formation), sediment material type and groundwater flow in the local area. Piezometers were arranged along transect lines (A-E) from east to west in the ponds as shown in Figure 1.

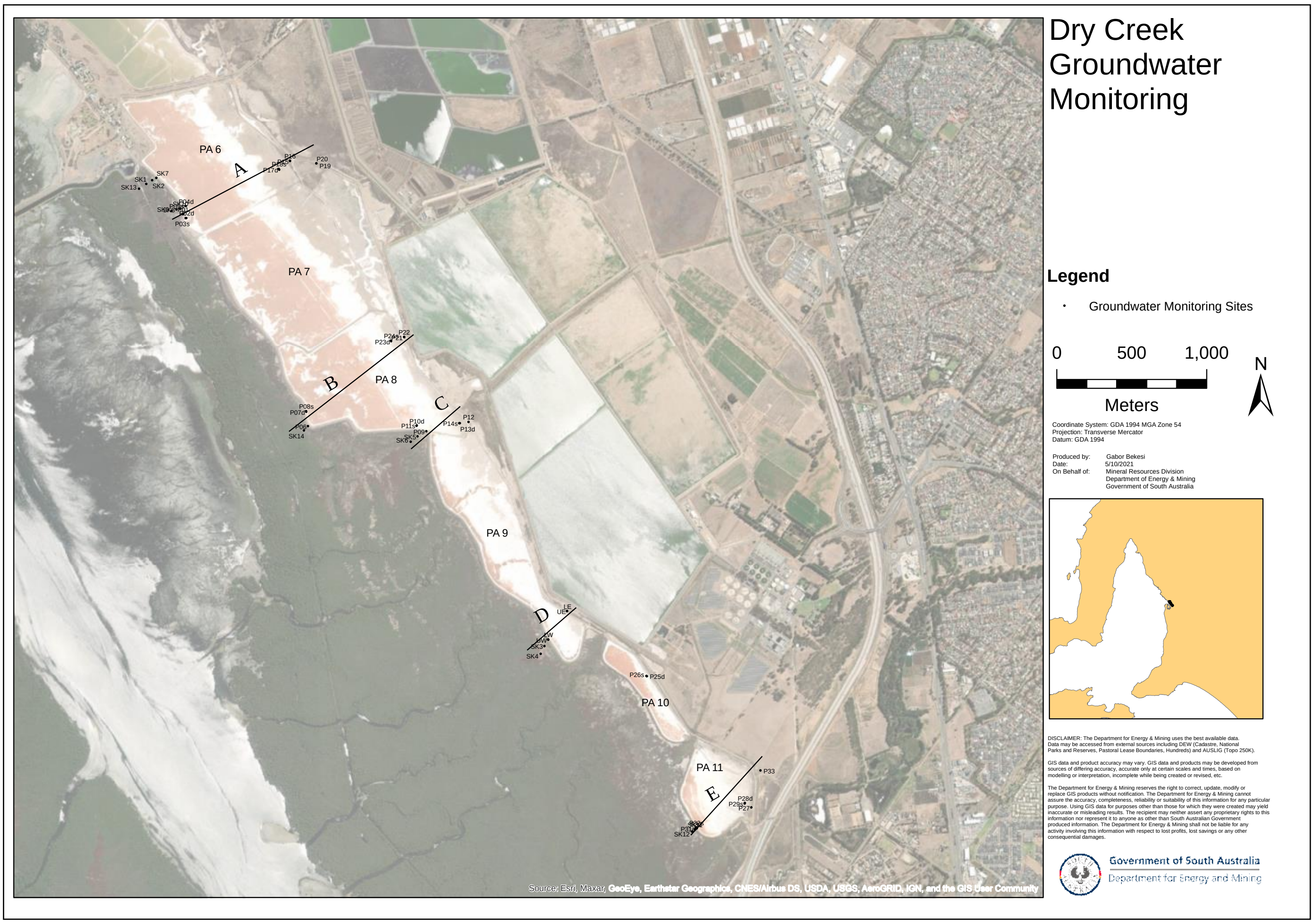

Figure 2: Transects of piezometers in Section 2 ponds PA6, PA7, PA8, PA 9, PA 10 and PA 11

There are two permeable layers below the ponds, *AQUIFER A:* upper gypsum gravel and confined to the pond, and *AQUIFER B* (St Kilda Formation): lowfer sand and shell grit layers and extends out under the bund wall and to the intertidal zone (refer to CSM 1 for more detail). These aquifers are separated by the peaty clay, which forms a semi-impervious layer. A downward gradient from the pond created an artificial groundwater recharge which has formed a groundwater 'mound' beneath the pond (DEM, pers comm).

The *AQUIFER A* is 0.1 to 0.6 m bgl[3] and consists of sulfidic gypsum gravels with high monosulfide contents, particularly on wetter low lying areas in the western portion of the salt ponds. The deeper *AQUIFER B* is 0.75 m bgl to 1.5 m bgl (approx.) and consists of sand and shell grit layers. Hydraulic head[4] data demonstrates that the groundwater flow direction of both aquifers is seaward from east to west/south-west (Tonkin 2015). Water tends to pool on the western segments of the pond surface due to topography of the pond (Tonkin 2015). The salinity of groundwater is related to surface water in the pond but it is likely that surface water and groundwaters within the aquifers are stratified[5] due to salinity and density gradients.

The base of the Section 2 ponds features a hard gypsum crust at the surface, which varies in thickness from 10 mm to 200 mm (Tonkin 2015). Tonkin (2015) found the degree of downward flow of groundwater (and thus the degree of recharge) through the crust to *AQUIFER A* below is determined by the thickness and durability of the surface crust (spatially variable) and the level of water above the surface (seasonally variable) (Tonkin 2015). The water level in the *AQUIFER A* was shown to increase during rainfall periods and then slowly decrease with evaporation and/or downward or lateral seepage (Tonkin 2015). When the salt evaporation ponds in Section 2 were drained and dried when salt mining ceased in late 2013, the gypsum crust surface changed from a hard continuous layer to a fragile, cracked, friable and discontinuous layer (See Fitzpatrick et al. (2014) for more detail). It our opinion, it is likely that this increased the downward flow of water compared to operation phases when the crust was relatively intact.

While there is a degree of hydraulic separation between the two aquifers due to the presence of a peaty clay semi confining layer (approximately 0.65-0.75 m bgl), vertical leakage can occur between the aquifers where the clay layer is discontinuous, where the clay layer thins out or where vertically structural features occur; such as old root channels or historical incising of old river channels and burrow pits[6] (Tonkin 2015). Vertical leakage through the semi confining layer to *AQUIFER B* would also increase when the hydraulic pressure in *AQUIFER A* amplifies due to pond surface water increases (i.e. when there is ponding or refilling of the ponds) (Tonkin 2015). There are several remnant creek lines in the ponds (visible on aerial imagery). These remnant creek lines adjoin tidal creeks outside the bund wall. The creek lines in the ponds represent depressions in the landscape, likely have coarser (more transmissive) and in our opinion would be areas of increase hydrological flow within the pond and under the coastal bund wall.

2.5. Bund Wall hydrology and leakage

The coastal bund wall embankments are constructed on marine sediments which were built from 'borrow pits located on either side of the bunds (Thomas 2010). Post-excavation, the borrow pits or 'scour areas' represent lower elevation areas in the landscape, as a result of removal of material to build the bund wall. The fill layers that form the bund walls are approximately 1.8 m thick and consist of layered and

[3] m bgl = Meters below ground level
[4] A measure of the level or pressure of the groundwater above a vertical datum (Australian Height Datum used in this report)
[5] Surface/groundwater present in layers of different salinity due to density
[6] A pit resulting from the excavation of material for use in embankments.

mixed shell grit and peaty clay material. Buried natural soils consist of peaty clay, carbonate sand and clay layers and have been shown to be permeable in some areas (Thomas 2010).

Water level fluctuations recorded with level loggers indicated high tide cycles influence groundwater levels at the coastal bund wall and within the salt ponds, when levels in the pond are lower than corresponding tide height (Tonkin 2015). These observations indicate that the hydraulic gradient can be reversed in the *AQUIFER B* (when tides are higher than pond surface water level). This data also illustrates the permeable nature of the sediments under the bund wall.

There is likely a 'zone of mixing' in the groundwater underneath the bund wall, where the hypersaline groundwater from the groundwater mound beneath the ponds mixes with the tidal water from the western side (Tonkin 2015). This zone of mixing would occur when the pond surface level is equal to or lower than the tidal range and would be more pronounced in areas where tidal influence is greatest, likely near remnant creek lines (in the pond) and tidal tributaries on the western side of the bund wall. The degree of mixing in the groundwater would be controlled by density effects, with more hypersaline groundwater potentially sitting above lower saline groundwater. When the pond surface water level is higher than tidal level, the prevailing direction of groundwater flow would be from the groundwater mound underneath the pond to the intertidal zone. In this case the salinities of the groundwater would be directly related to the salinity in the pond surface water. When the pond level is lower than the tidal level, the groundwater would be a mix of pond salinity and tidal salinity, and lower in salinity (Tonkin 2015).

Aerial imagery from the operation phases (2009) illustrates the presence of salt scalds and/or saturated surface ponds in the intertidal zones immediately to the west of the bund wall near PA 7 (Figure 3 (a)). The salt scalds/sediment saturation suggest that groundwater mounding and leakage under the bund wall was present when the ponds were operational. Imagery from the same area in 2019 (Figure 3 (a) Intertidal area directly adjacent PA 7 in 2009 illustrating salt scalds and (b) Intertidal area directly adjacent PA 7 in 2019 indicating vegetation condition improvementFigure 3 (b)), after the pond had dried, demonstrate a recovery in the intertidal saltmarsh zone immediately adjacent the bund wall. The lower pond level during the drying period would have likely reduced the hypersaline groundwater seepage from the pond to the intertidal zone, allowing tidal flushing to dilute soil pore water salinities sufficiently that saltmarsh vegetation was able to re-establish. Alternatively, the lower groundwater head may have replaced permanent sediment saturation with cycling between saturation and unsaturation, allowing vegetation reestablishment.

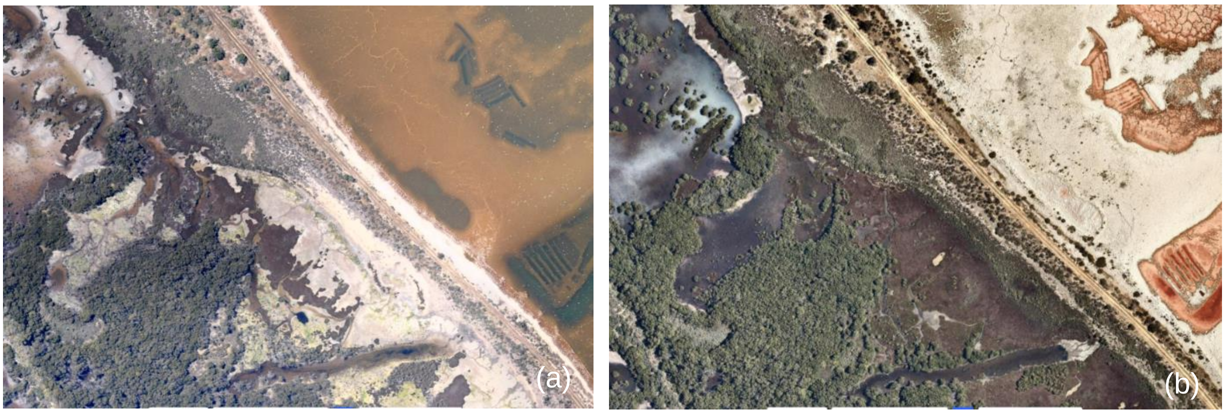

Figure 3 (a) Intertidal area directly adjacent PA 7 in 2009 illustrating salt scalds and (b) Intertidal area directly adjacent PA 7 in 2019 indicating vegetation condition improvement

2.6. Minerology of Section 2 following drying

The evaporation of a water body allows the concentrations of dissolved components in the solution, to a point where when mineral precipitation occurs. Different minerals precipitate at different stages of evaporation. During operation, the ponds in Section 2 were evaporated to the point where gypsum ($CaSO_4.2H_2O$) precipitated, and the pond surface was dominated by crusts of this mineral.

Following the closure of Section 2, and subsequent drying phase, Fitzpatrick et al. (2014) found that the soluble salts on the surface of the ponds in Section 2 had become dominant in both halite (NaCl) and gypsum, as well as other minerals such as calcite and elements such as Magnesium. The drying phase changed the surface minerology of the salts on the surface of the pond in Section 2 (Fitzpatrick et al. 2014). The subsequent summer evaporation and re-dissolution of salt during winter rainfall periods led to higher concentrations of salts in the overlying pooling water, and dominance in halite (Fitzpatrick et al. 2014). The presences of halobacteria and the alga *Dunaliella* (pink colour on the surface of the ponds, from aerial images) between 2015 to 2019 is further evidence of halite precipitation on the pond surface in Section 2. Fitzpatrick et al. (2014) noted a change in the surface of Section 2, from a hard, continuous crust to one which was more fragile and discontinuous after pond drying and then a heavy rainfall event in 2014. The concentration of salt on the surface, combined with pooling of lower salinity winter rainfall, may have facilitated additional gypsum crust dissolution in the following summer and winter periods, but there is no direct scientific data of additional surface cracking resulting from gypsum dissolution in Section 2 from 2015-2019.

2.7. SA Water trial and chemistry in Section 2

From December 2014 to 2018, SA Water used PA 9 and PA 10 (Section 2) to trial denitrification of wastewater from the Bolivar treatment plant. Geochemical modelling work completed by Water Quality Science before the trial initiated, quantified the expected changes to the gypsum crust under different ionic concentrations. This work found that the dissolution and precipitation of gypsum would be minimal in order to achieve equilibrium with the surface water, given the low pond surface water volume (Mosley 2014).

In 2014, wastewater from the treatment plant filled PA 9 (Stage 1) and in 2015, both PA 9 and PA 10 were filled (Stage 2). Salinity monitoring in the ponds illustrated the stage two refilling of PA 9 and PA 10 took several months to stabilise salinity, with TDS fluctuating around 60 g/L. When flows into the pond stopped over summer, evaporation quickly increased in PA 10 with salinities from above 100 g/L to as high as 140 g/L. When flow back into the pond recommenced, salinities decreased between 40-60 g/L, stabilising to acceptable salinity within 3 weeks (SA Water 2016).

Monitoring of the average ion concentration in ponds PA 9 and PA 10 confirmed that the equilibrium ion values were within the target outlined in the geochemical model to ensure only minimal gypsum crust dissolution (0.2 cm per year from the gypsum crust) (SA Water 2016).

Groundwater adjacent the PA 9 and PA 10 ponds was also monitored during the trial (in *AQUIFER B*) and TDS measurements used as an indicator of seepage from the trial site to the adjacent intertidal area. The TDS in the piezometers to the western side of the bund were between 100 – 150 g/L TDS at the beginning of the trial, and trended lower over the course of the trial to around 50 g/L TDS. This indicates that seepage was present under the bund wall in this trial (as it was likely present during the operation phase), but the salinity of the groundwater was lower (due to dilution with the reduced salinity of incoming wastewater from the treatment plant). The pond level was also kept low (with the aim of maintaining a wading bird habitat and encourage evaporation over groundwater lateral flow) and the crust dissolution was minimal resulting in a low hydraulic head pressure through any preferential flow pathways and aquifers below the ponds. This, combined with a relatively intact crust surface (as ion composition remained in target concentrations for minimal dissolution) and lower salinity levels, meant seepage into the intertidal zone from the ponds did not additionally affect vegetation communities (as observed from aerial imagery).

In 2018, the trial expanded and wastewater was pumped into PA 8. Monitoring allowed the assessment of both groundwater levels and salinity in the westward bund wall and ion concentration in the pond level. All were within target ranges (SA Water 2016). Ponds PA 8, PA 9 and PA 10 dried out in summer 2019.

2.8. Pond scale hydrology and salinity in Section 3

During the operational phase (prior to 2013), seawater flowed through the different ponds in Section 4 and 3, concentrating along the passage north to south. Salinity increased from 35 g/l near the inlet at Middle Beach to around 160 g/L at the final pond in Section 3, PA 5. Salinity was kept within a relatively stable range during the operation phase (Figure 4).

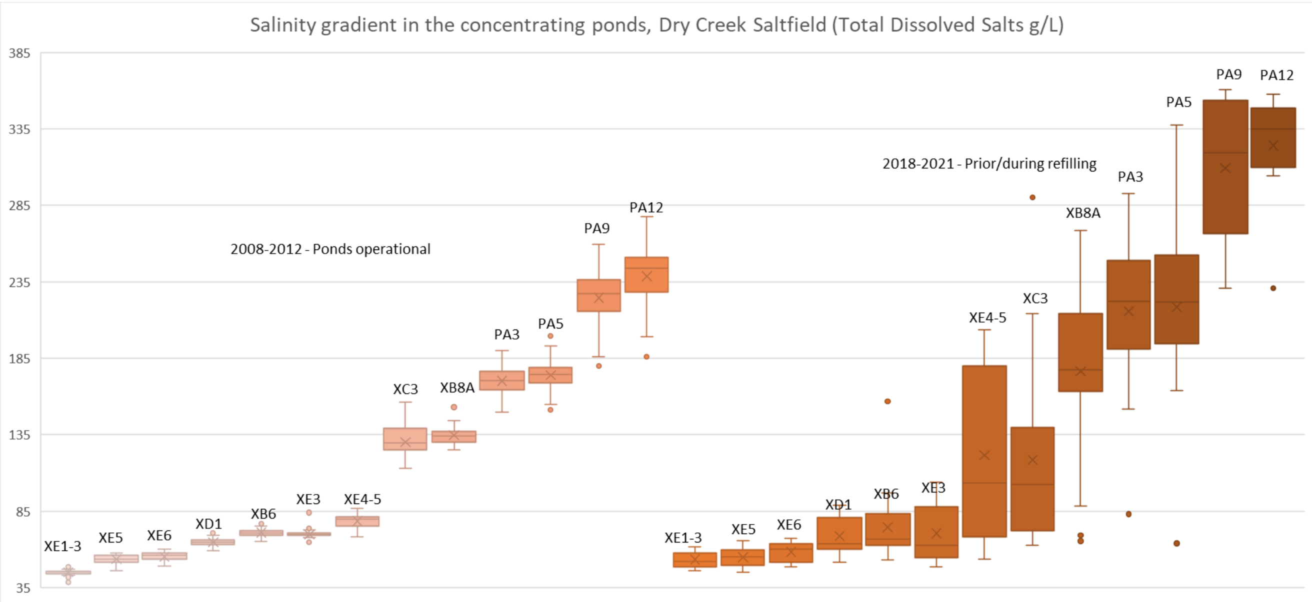

Figure 4 : ***TDS (g/L) of the ponds in all ponds in Section 4, 3 and 2 during operation phase vs holding pattern (graph adapted from historical data and report from Save St Kilda Mangroves Alliance (2021))***

When the temporary holding pattern was established at the site in late 2013, seawater continued to flow through the ponds of Section 4 and 3, from north to south. Once in PA5, brine was then discharged into the SA Water outfall (Bolivar Channel) using temporary discharge arrangements. Mixing the brine with the water from the Bolivar Channel, allowed sufficient dilution for discharge into the Barker Inlet (limited of 45 g/L TDS as set by the SA Environment Protection Authority).

Seasonal fluctuations and episodic reduction in the flow rate from the Bolivar wastewater plant (due to diversion to the Northern Adelaide Plains Irrigation Scheme) reduced the amount of water available for dilution from PA5, meaning less brine was able to be discharged through the channel at certain times during the year (primarily the summer months). This appeared to become particularly problematic in late

2018 and in 2019. The salinity along the pond chain in Section 3 not only increased but also fluctuated substantially over this time, due to variable brine movement and control though the pond chain.

The increase in salinity is demonstrated in Figure 5, which shows data from PA3, PA5 and PA 9, from both the operation phases (blue rectangle - 2008 to 2012) and the subsequent holding pattern phase (red rectangle 2018-2021). PA3 and PA 5 increased from average ~160 g/L TDS (1.11 SG) to ~215 g/L (~1.14 SG) during the holding pattern.

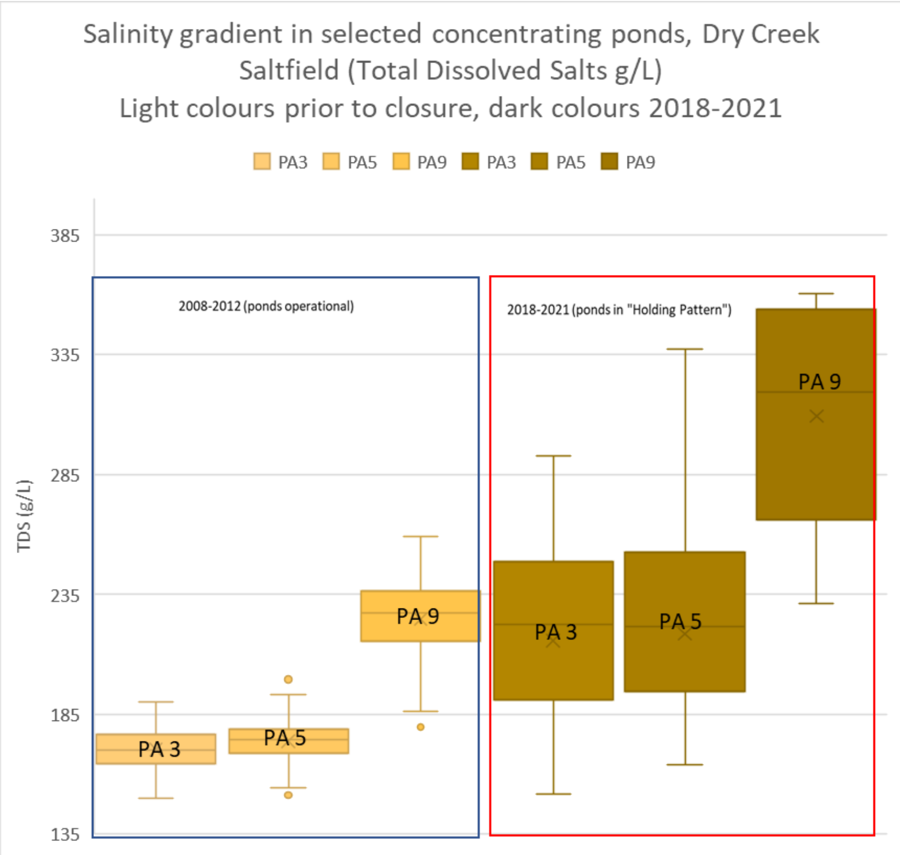

Figure 5: ***Salinity (TDS g/L) in PA 3 and PA 5 (Section 3) and PA 9 (Section 2) during operation phase (2008-2012) compared to the holding pattern (2018-2020 data shown here) (graph adapted from historical data and report from Save St Kilda Mangroves Alliance (2021))***

Figure 6 shows the TDS in PA 3 and PA 5 ponds for sampling conducted between 2008-2012 and post 2019. The degree of seasonal variability in the TDS is apparent, with particularly high increases in salinity over the summer months in the immediate period before refilling commenced in December 2019

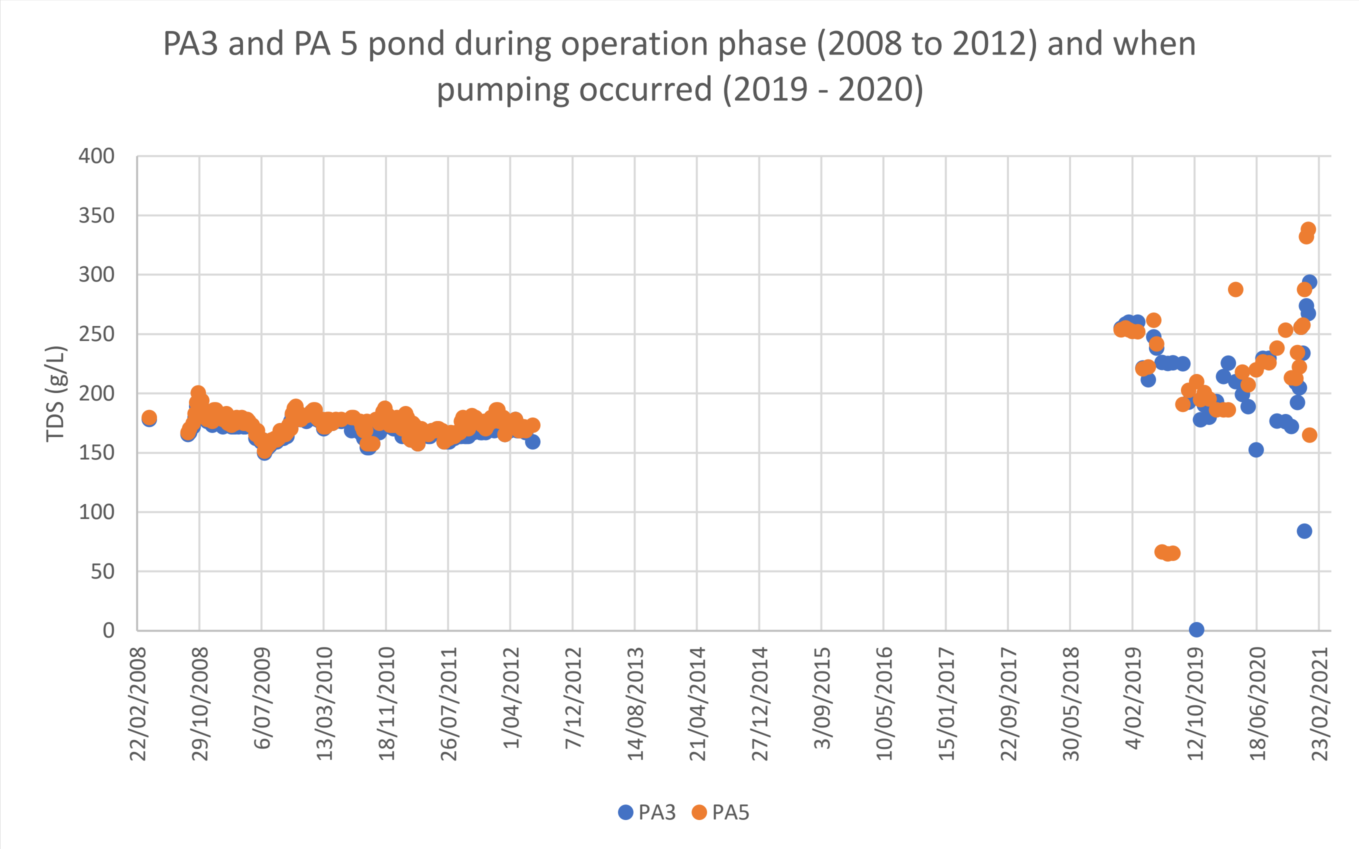

Figure 6 ***TDS (g/L) of PA 3 and PA 5 ponds in Section 3 (graph adapted from historical data)***

In Figure 6, the larger range in salinity values in the ponds Section 3 (particularly those the southern part of Section 3) is evident during the holding pattern phase, when compared to salinity ranges during the operation phase. This is also clear in Figure 6 above.

From late December 2019 and during 2020, brine was discharged to both the SA Water Outfall but also discharged into Section 2 (PA 6, PA 7, PA 8, PA 9 and PA 10). The ponds were filled to a level of approximately 2 m AHD in PA 6, 7 and 8. The purpose of this as stated in the Program of Environmental Protection and Rehabilitation (written after impact occurred) (PEPR) (BDC 2020) was;

- *To keep the overall discharge from PA5 sufficient to manage the environmental quality of the brine ponds between Middle Beach and PA5; and*
- *To make brine available for pumping from the southern end of Section 2 into Section 1 to enable the planning and design of the resumption of commercial salt production*

It is important to note that the salinity entering Section 2 in late December 2019 in through 2020, was of a much higher salinity (mean above 200 g/L TDS) than that during production time (mean approximately 160 g/L TDS) (Figure 6).

3. Refilling of Section 2

3.1. Hydrology – increase in hydraulic gradient following refilling of Section 2

During the pond refilling in late 2019, surface water elevation in the ponds PA 6, PA 7, PA 8, PA 9 and PA 10 increased up to 2 m AHD, compared to 1.3 m AHD when ponds were dry. There was a significant increase in recharge to the groundwater in *AQUIFER A* and *AQUIFER B* which amplified the groundwater mound below and adjacent to the pond.

Monitoring data, collected on 26 November and 21 December 2020, indicate that groundwater heads in piezometers (P01, P02, P03, P04, P05) in the western part of salt pond PA6 were 0.7- 0.8 m above those in 2014 (Table 4 and Figure 7). As the receiving *AQUIFER A* and *AQUIFER B* are both relatively thin aquifers, the change of 0.7 m from 2014 values represents a significant increase in saturated aquifer thickness (DEM, pers comm).

This elevated groundwater head under the pond in turn increased the hydraulic gradient (flow of water from area of high hydraulic head to an area of lower hydraulic head) both towards the western side of the pond and the adjacent intertidal zone. There was also an increased hydraulic gradient towards the eastern landward side of the pond as evidenced by piezometers in the eastern side of the pond.

Table 4 ***Increase in hydraulic head (m AHD) at selected time periods from the pond, on the bund and in the intertidal zone.***

	Hydraulic head (m AHD) in pond (western side) (P02)	Hydraulic head (m AHD) in pond (western side) (P04)	Hydraulic head (m AHD) in west bund wall (P01)	Hydraulic head (m AHD) in intertidal zone (SK 8)
April 2014	**1.21**	**1.14**	**0.95**	**n/a**
November 2020	**2.00**	**1.94**	**1.55**	**0.98**
December 2020	1.94	1.68	1.41	1.08
February 2021	1.62	1.51	1.25	0.88
April 2021	1.44	1.29	1.28	0.95
June 2021	1.42	1.30	1.29	0.84
August 2021	1.57	1.47	1.10	1.17
December 2021	1.43	1.29	1.13	0.96
April 2022	**1.19**	**0.95**	**1.06**	**0.76**

In late 2020, a series of monitoring wells were installed in the intertidal zone to align generally with the existing transects. The amplification in hydraulic head in Transect A between piezometers in the pond (P0 2 and P0 4), the western bund wall (P0 1) and the intertidal zone (SK 8) can be clearly seen when the ponds were at their highest in 2020 and early 2021 (Table 4). Figure 7 represents the piezometric surface from east to west along Transect A (see Figure 2: for location). The difference in gradient between the refilling phase, the reference period (2014) and the pumping stage are evident.

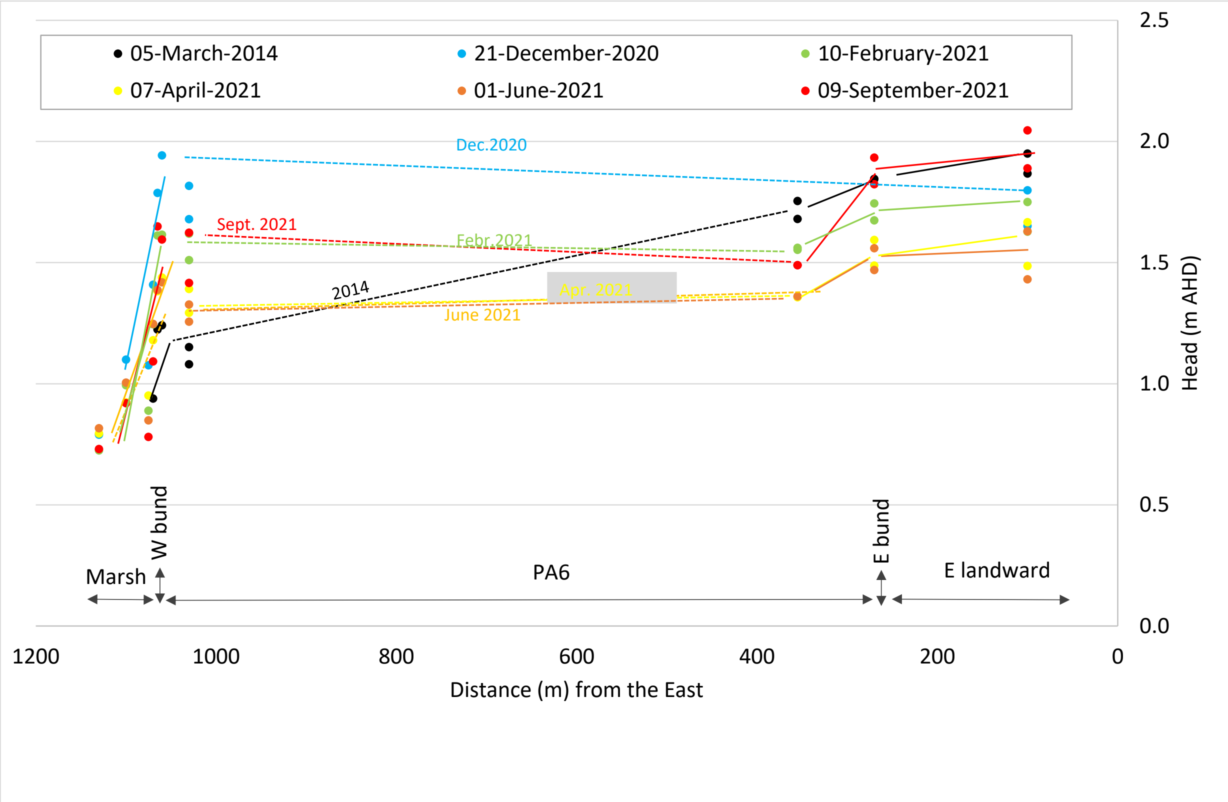

Figure 7: Change in hydraulic head (m AHD) along Transect A, demonstrating degree of hydraulic head change between 2014 (black line) and the period of refill (Blue line: 21st December 2020) and then after pumping, green February 2021, yellow line: April 2021, orange line: June 2021, red line: September 2021 (graph from DEM)

The factors which lead to the increase in hydraulic head and groundwater flow towards the intertidal zone include;

- the Section 2 pond level increase in late 2019 to 2020; the pond surface water level following the refilling period was higher than at any time since the operation phase
- the interim period of drying and rewetting between 2014 – 2019 which likely changed the chemistry of the gypsum crust, allowing increased recharge through the crust and through the bund

When the brine was moved out of Section 2 in 2021, and as it evaporated over summer, the hydraulic head difference between the pond and the intertidal zone decreased significantly (Table 4, Figure 7) and the groundwater flow through the aquifers beneath the pond to the intertidal zone would have slowed.

When examining movement of groundwater in this context there are several important factors to note (DEM, pers comm):

- Groundwater flow is assumed to occur as a result of a hydraulic gradient. However, there is also a density contrast, between the groundwater beneath the ponds and groundwater below the marsh, that can drive purely density driven (convective) groundwater and salt flow.
- The data from the piezometer well examined at the site represent the salinity of the entire aquifer (as they are screen across a depth interval). It is likely that variation with depth would occur, due to salinity differences and differences in soil composition and properties.

- It is assumed that the hydraulic conductivity of the aquifer is homogeneous. It is likely the aquifer(s) may be heterogeneous.
- The piezometers in the intertidal zone did not extend into the mangrove zone along Transect A and did not spatially cover a range of elevations and/or sediment types. This was due to access issues making spatial coverage of piezometers limited.

3.2. Chemistry – transport of salt to the groundwater and intertidal zone

The salinity of the pond water in Section 2 following the refilling phase was significantly higher than during operational times due to two factors:

- Brine pumped from Section 3 into the ponds in Section 2 was a higher salinity than during the operation phase (see Figure 6) due to the complexities discussed in section 2.6
- When the ponds in Section 2 were refilled there would have been dissolution of soluble salts (in particular NaCl) that had built up in the drying/wetting phases from 2014-2019. This led to a further increase in the salinity of the pond water as salt at the pond surface dissolved until equilibrium with the overlying water was reached.

As the pond refilled, the brine in Section 2 became extremely hypersaline (>300 g/L TDS), indicating a NaCl-dominated brine (Lionberger et al. 2004). As the brine moved from the pond down through the crust to the groundwater mound beneath, the groundwater became extremely hypersaline. This hypersaline brine then moved towards the intertidal zone under the increased hydraulic gradient discussed in Section 3.1.

Evidence from work done by DEM (pers comm 2022) demonstrated that extremely hypersaline groundwater would have likely originated from the pond surface recharge, rather than any regional groundwater input. The regional groundwater in bores 2 km and 10 km from the site show brackish to mildly saline groundwater (12 g/L TDS (10 km) and 15 g/L TDS (2 km)) (Table 5) (data from WaterConnect). This is distinct from the groundwater salinity in the piezometers near Section 2 which is more than 100 times larger than that of the 2km data (and more than 150 times larger than the median for the 10km dataset) (DEM, pers comm) (Table 5).

Table 5: ***TDS Data from regional bores compared to local monitoring at Dry Creek***

Data	No of observations	10%ile TDS (mg/L)	50%ile or median TDS (mg/L)	90%ile TDS (mg/L)
Regional <2km	32	855	1500	2148
Regional <10km	2670	651	1177	4477
Salt fields - Dry Creek Monitoring	392	85510	181587	309900

Data collected in 2014 (Tonkin 2015) gives an indication of the salinity of the aquifers below the pond and under the bund walls before the refilling and allows a comparison to the salinity following refilling and subsequent pumping phase. Only data from the western edge of the pond in PA 6 and western bund is shown here (Figure 8), but data from the eastern side of the pond and bund wall is available, as is data from other ponds in Section 2.

The salinity in both the pond piezometers (P02 and P04) and the bund wall (P01) increased substaintially when the ponds were refilled (compared to the reference period in 2014. As pumping commenced in 2021, the salinity of the bund wall decreased (P01, Figure 8) and the hydraulic head pressure in the pond and to the groundwater mound decreased. It is likely that the zone of mixing (discussed in section 2.5) under the bund wall was able to reestablish, as the hydraulic head pressure from the pond to the salt marsh decreased. However, the groundwater beneath the pond remains extremely hypersaline saline (P02 and P04, Figure 8).

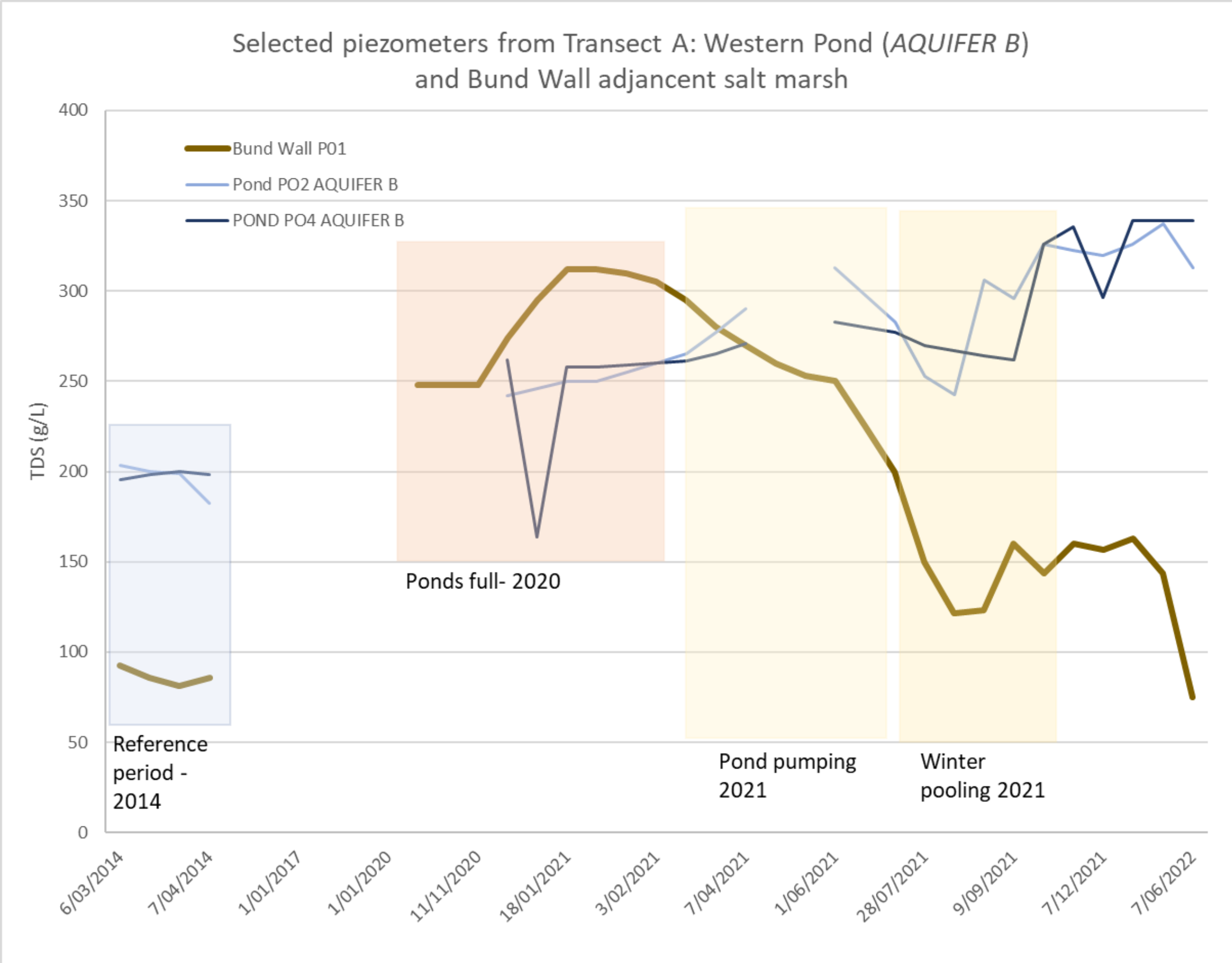

Figure 8: ***Change in salinity between the 2014 reference period and the increase in salinity from the earliest monitoring in November 2020. Only data from AQUIFER B is shown here for ease of interpretation. AQUIFER A results showed a similar trend but TDS was higher*****.**

Both the level of pond water (and hence hydraulic gradient in the groundwater) and the increased salinity (higher than that during the operation phases) are important factors when examining the transport of extremely hypersaline water to the intertidal zone.

Additional work has been done by DEM to develop a ‘salt index’ for Transect A which aims to tracks changes over time of a ‘salt flux’ from beneath the pond in PA 6 to the intertidal zone. The index is calculated from groundwater head measurements and salinity at seven sites within the pond, and salinity and groundwater head measurement from one well in the bund, P01. Groundwater heads are corrected to density and the influence of viscosity is incorporated into the Transect A salt index. The Transect A salt index is based on several assumptions, and it represents a simplified single quantitative measure of the complex trends in salt flux near Transect A. The Transect A salt index is entirely based on existing measurements and is not a predictive (model) tool but has been used to understand seasonal and longer-term trends in the ‘salt flux’ moving towards the intertidal zone. The Salt Index work is discussed in detail in Appendix 1. In summary, from November 2020 to June 2021 the data demonstrates was a steep decline in the Transect A salt index (100% to 40%) salt index due to pumping from Section 2 and the summer evaporation. The decline in the salt index has been noted to be primarily due to a decline in the hydraulic head. From June to November 2021 there was an increasing head difference due to winter rain pooling. The reduction in salinity (most likely a result of tidal influence in P01, as discussed in section 2.5 above) allowed the Transect A salt index remained stable around 40%. From November 2021 to April 2022 the Transect A salt index decreased again from 40% to 25%. This was again likely due to decreasing head difference (summer lack of rainfall and high evaporation) and stable salinity in this piezometer P 01.

It is acknowedged by DEM that the salt index is not a model, rather a identifier of change (‘salt flux’) in the piezometers along transect A. Limitiations exist with the salt index, primarly with the use of a single piezometer P01. This site is known to be influenced by both the groundwater from the pond and tides when the pond level is low, as discussed in section 2.5. It is possible that salt could still be exported to the intertidal zone, but it is being diluted at this particular peizometer by tidal waters, giving an erroneous indication of the movement of salt towards the marsh. This is a particularly important as the pond piezometers (P02, P03, P04, P05) demonstrate that highly saline water is still present in the aquifers below the surface. Additional data from other peizometer transects could further constrain salt movement from the ponds in Section 2 to the intertidal zone. The data collated (by the EPA) from piezometers installed in 6 transects across the saltmarsh from PA6-11 is currently unavailable for wider dissemination and use while the EPA completes its investigation and completes any regulatory action related to this work (EPA, pers comm).

4. Hydrological, chemistry and vegetation changes in the Intertidal zone

4.1. Salinity in the intertidal zone post impact

Previous work completed by Thomas (2010) illustrated EC (measured as 1:5 ratio) of the sediment in the mangrove areas west of the boardwalk bund ranged from 46.8 dS/m (approx. 35 g/L) closest to the boardwalk, to 22.0 dS/m (approx. 16 g/L TDS) in the central seaward area of the mangrove forest (Figure 1). Data in Dittmann et al. (2022) records porewater salinities in 3 zones west of the boardwalk bund (mangrove vegetated area) as having salinities from 35 psu (~35 g/L) to 50 psu (~50 g/L), with higher values closer to boardwalk bund). No other data appears to exist for soil EC in the intertidal zone between the new bund wall and the boardwalk bund prior to impact.

Piezometers were installed in the intertidal zone to the west of the Section 2 bund in November 2020 following observations of vegetation dieback. The piezometers align generally to the existing piezometer transects (SK 8, 9, 10 – Transect A, SK 5 and 6 – Transect C, SK 3 and 4 – Transect D (Figure 1 and Figure 9). Additional piezometers were installed in the saltmarsh intertidal zone between the boardwalk bund and Section 2 bund immediately south of the marina (SK 1,2 and 7) and west of the boardwalk bund (Figure 9). Piezometer SK11 and SK 12 were installed adjacent to PA11 and SK13 adjacent to PA8 as additional transects across unaffected and affected parts of the saltmarsh/mangroves.

Figure 9: ***EPA piezometer location map***

Data from piezometers near Transect A (SK8, SK 10 and SK 9) in 2020, demonstrate high salinity (>250 g/L) in the intertidal zone during the time when the surface water in the Section 2 ponds was high (Figure 10). The decrease in salinity in piezometers SK 8, and SK 10 following pond pumping and water level lowering over summer is evident in March 2021. As discussed above in section 2.3, there is likely a zone of mixing under the bund wall separating the Section 2 ponds, where tidal water mixes with groundwater flowing from under the pond. Once the hydraulic head pressure from the ponds towards the intertidal zone decreased, tidal mixing was likely able to exert more influence on these sediments, reducing the salinity over time. In the piezometers closest to the Section 2 bund, salinity reduces significantly over time to below 100 g/L, although sediments in SK9 remain above 100 g/L. This is quite high for these sediments and would likely be a sedimentary environment where vegetation would struggle to recolonise (Dittmann et al. 2022).

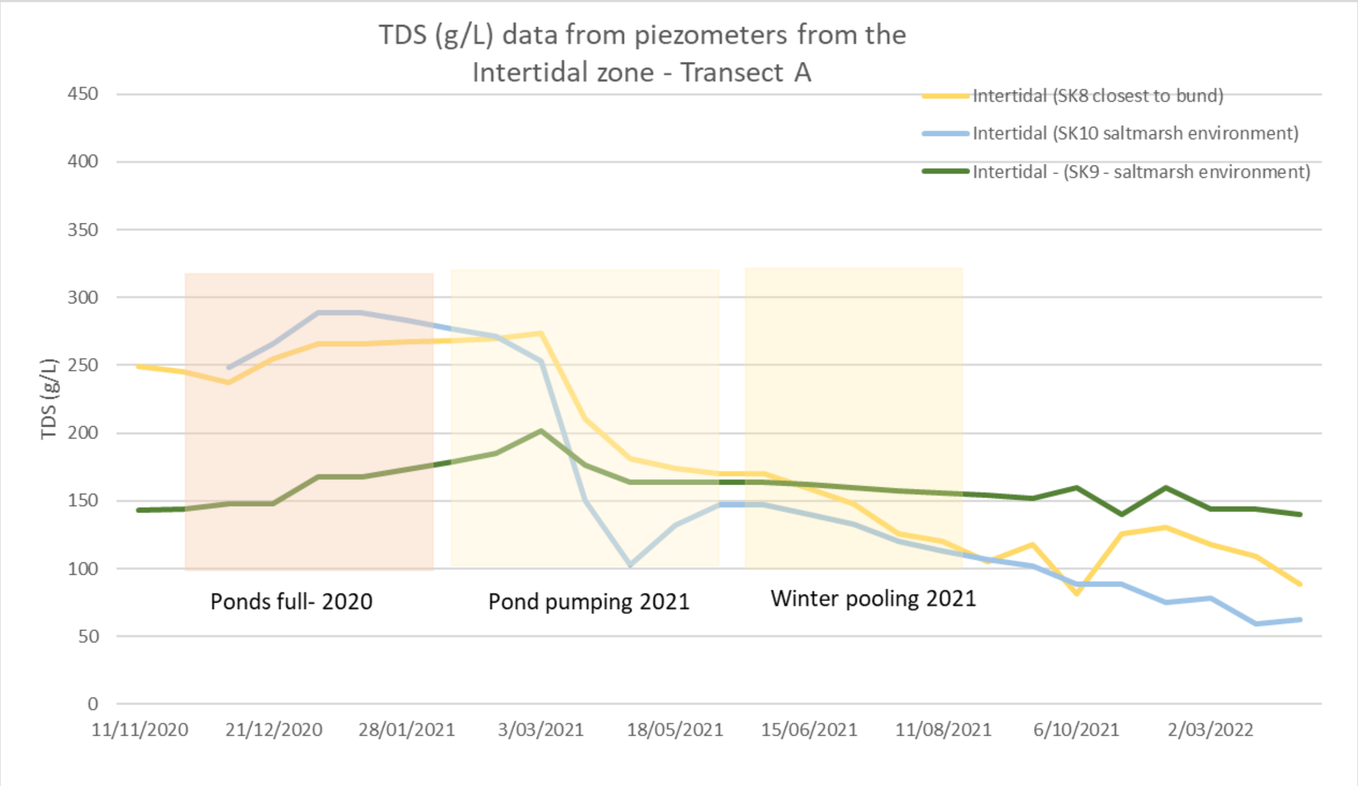

Figure 10: Piezometer data from the intertidal zone (Transect A – SK8: saltmarsh environment 50m from bund, SK 10: closest to the bund and SK 9: saltmarsh environment, 100m from bund).

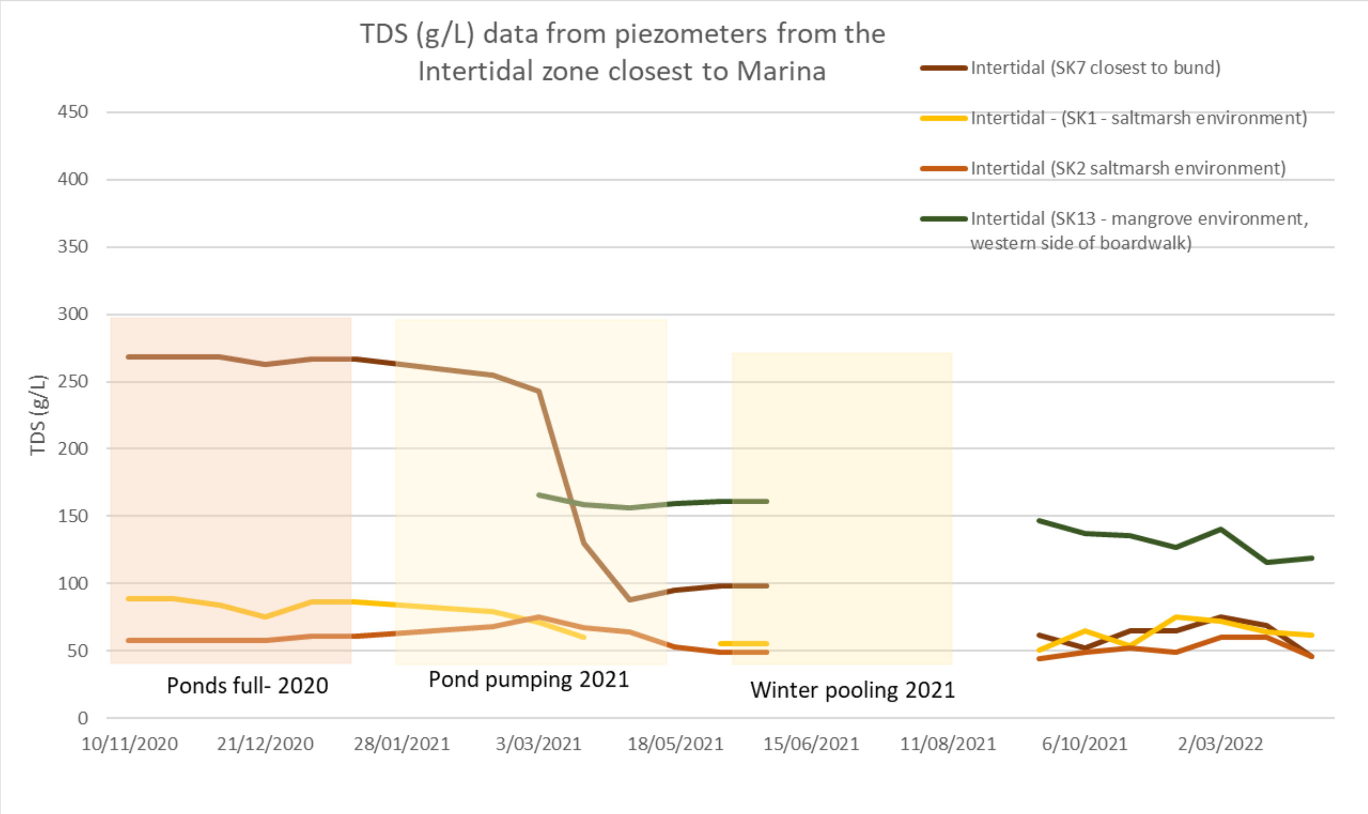

Figure 11: Piezometer data from the intertidal zone closest to the Marina (SK7: Side of the bund wall, SK 1: saltmarsh ~50 m from bund and SK 2: saltmarsh 30 m from the bund, and SK13: mangrove environment western side of the boardwalk).

Figure 11 shows data from the intertidal zone immediately south of the Marina between the Section 2 bund and the boardwalk bund (see map Figure 9). The high level of salinity in SK 7 (closest to the bund) can be seen during 2020 and early 2021. This is a result of this piezometer being on the seaward side of the bund wall. The decrease in salinity is also evident in SK7 following the pumping and evaporation from the pond in early 2021. SK1 also declines in salinity after pumping commences, however, SK2 remains relatively stable over time, and was not extremely hypersaline during the monitoring period. SK13, which is in the mangrove zone remains > 100 g/L during the data collection period.

This data indicates that there is a likely relationship between the distance from to the Section 2 bund and the sediments affected by the extremely hypersaline groundwater from under Section 2. The data also suggests a degree of variability in the response of the intertidal zone to the hypersaline brine leakage. Elevation difference and/or sediment type in the intertidal zone are likely factors which control the where the extreme hypersaline water leaking from Section 2 accumulates, as well as ability of the soil profile to be adequately flushed by the tide.

The higher elevation areas in the intertidal zone are more likely to be on the chenier ridges (sandy/shelly, coarser material), whereas the lower elevation areas are more likely to be mudflats (muds/clays, finer material) (Thomas 2010). Coarse material will likely leach and flush salt faster than finer, muddy sediments. The elevation would also contribute to draining/flushing compared to lower elevation sediments which can accumulate salt more readily s they have limited draining/flushing. This was supported by hyperspectral datasets from DEW (Department for Environment and Water 2021b), which demonstrated a link between elevation data and vegetation loss, suggesting topographically driven drainage and flushing across tidal flats and creeks impacted the Normalised Difference Vegetation Index (NDVI) which determines vegetation loss (more detail in section 4.3 below).

Work done in an Honours Project by The University of Adelaide (student Lucy Wood, supervisors Dr. Alice Jones and A/Prof. Luke Mosley) further illustrated the complex nature of the intertidal zone by examining porewater salinities in different sediment types, at high and low elevations and at different distances from the Section 2 bund. The work related these factors to the proportion of vegetation dieback in surveyed quadrats (Wood 2022).

The work, completed during 2021 and early 2022, examined 3 transects of 5 sites each in the affected saltmarsh areas between the Section 2 bund and the boardwalk bund (all transects here were from several affected sites) and an additional 3 transects (2 affected and one healthy) of 5 sites in the affected mangrove zone west of the boardwalk bund (Figure 12). The results were highly variable spatially and temporally, again highlighting the complex nature of the sediments in the intertidal zone. Vegetation quadrats with finer sediments (mudflats) recorded more dieback and were higher in salinity compared to sediment with coarser sediments (old chenier ridges). Similarly, quadrats closer to the bund wall and those with lower elevation also recorded more dieback and were higher in salinity that sites further from the bund wall and sites higher in elevation. Sediment type (coarse or fine), elevation (high or low) and distance from the bund (close or far) were all found to have contributed to the proportion of saltmarsh dieback (Wood 2022).

Figure 13 (a) and (b) show the linear mixed effects models developed from the data. The models demonstrate these key drivers of soil porewater salinity at the sites which were sampled in this study. As these plots show, distance from the bund wall (a) and elevation (b) were significant predictors of porewater salinity at the sites selected. As coarse sediments are more likely on the higher elevation areas (chenier ridges) and finer sediments are more likely on lower elevation areas, sediment type can also be a predicter of increased porewater salinity.

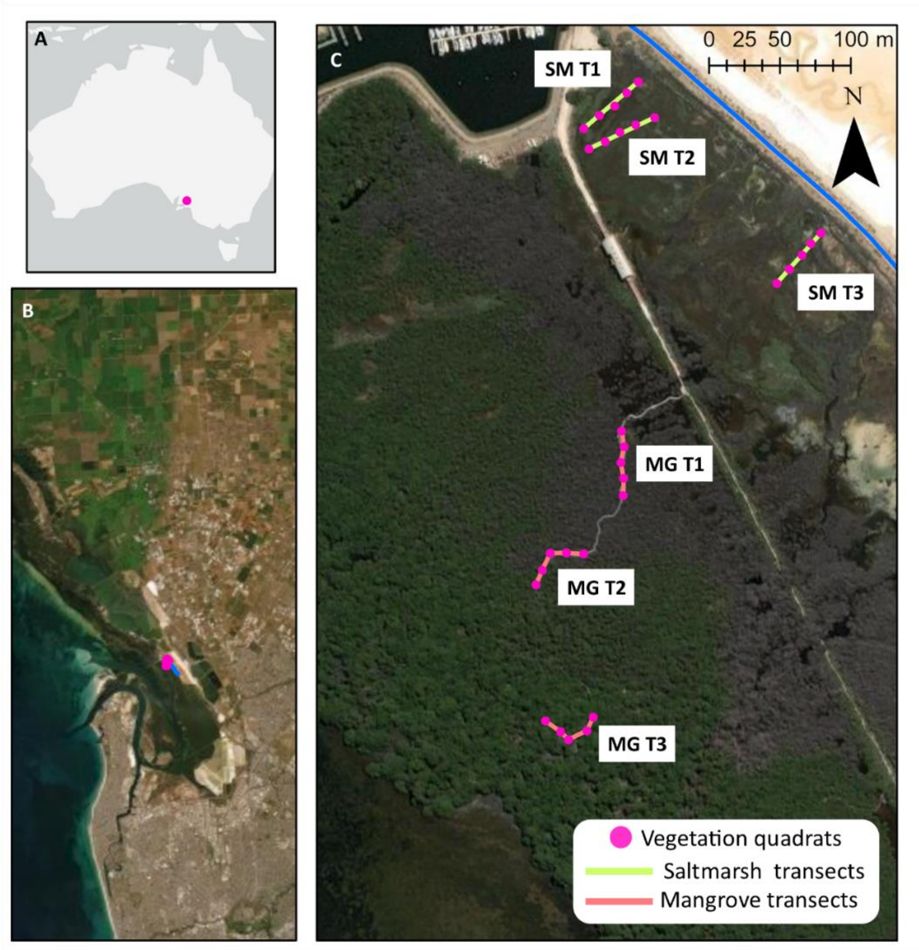

Figure 12*: vegetation transects and quadrats from work done by The University of Adelaide (Lucy Wood, Dr Alice Jones and A/Prof Luke Mosley)*

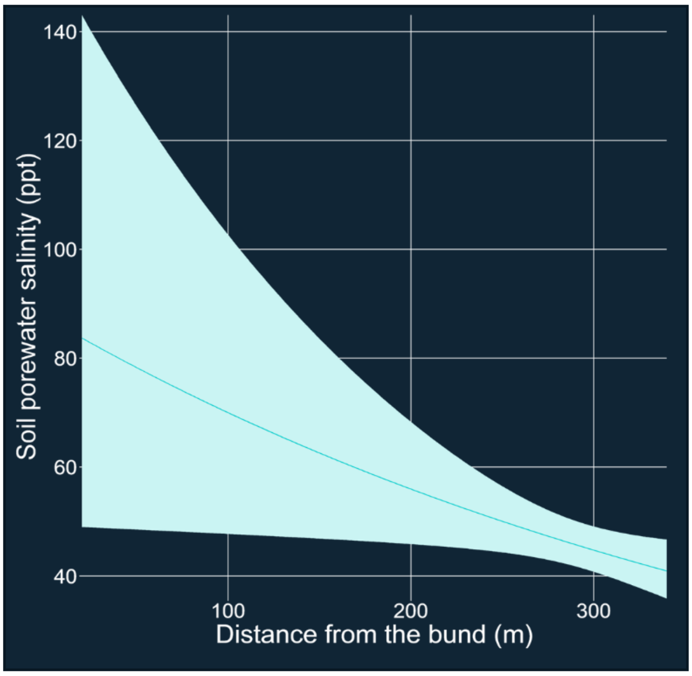

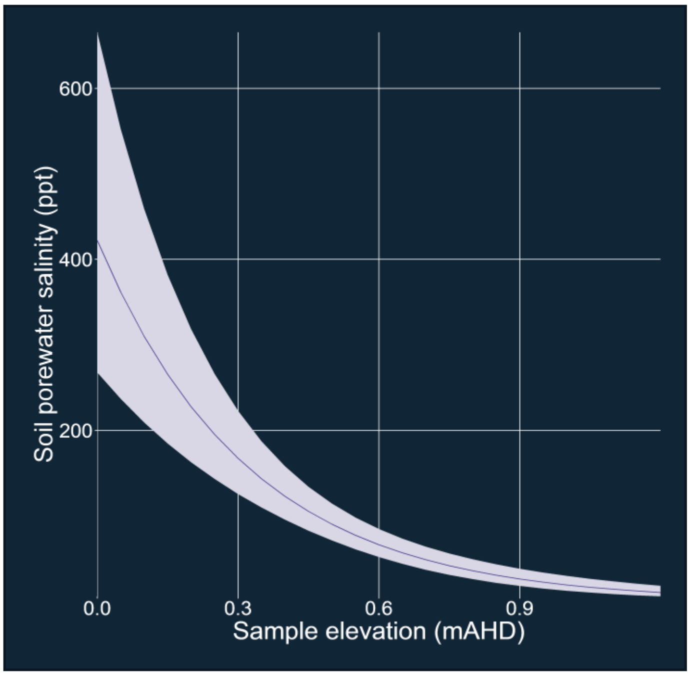

Figure 13 (a) and (b): Linear mixed model effects of porewater salinity (ppt) to (a) distance from the bund and (b) sample elevation. Model R2 = 0.43, mean prediction error = 19.3 ppt, ***from work done by The University of Adelaide (Lucy Wood, Dr Alice Jones and A/Prof Luke Mosley)***

Importantly, porewater salinity in some areas was found to be still elevated in January 2022, indicating some sediments are likely still affected by hypersaline brine in the system. This work highlighted the variability in salinity in the intertidal zone and underlined that more data is needed to constrain which sediments remain hypersaline.

In 2022, Dittmann et al. (2022) reported on findings from a multidisciplinary investigation in the mangrove area at the site (west of the boardwalk bund) which combined airborne remote sensing with on-ground measurements. This study classifies “healthy,” “stressed,” or “dead” mangroves (from remote sensing, Normalized Difference Vegetation Index – ‘NDVI’) to infield measurements photosynthetic traits, CO_2 efflux from the sediment, salinity, soil redox potential and sulfate and chloride concentration (Dittmann et al. 2022).

This study mentions that higher concentrations of salt with depth (> 100 g/L or 90 psu) in the soil profile are consistent with upward seepage arising from an elevated head of hypersaline groundwater (Dittmann et al. 2022). The salinities of the surface water in the mangrove ecosystem were lower (54-65 g/L or 50-60 psu) which was consistent with flushing with seawater via tidal action. Flushing was found to be stronger at the seaward side of the forest where it would buffer mangrove from the development of hypersaline conditions in porewater. This was found elsewhere (Lovelock et al. 2017). The mangrove forest adjacent the boardwalk bund (site closest to Section 2) would have less frequent inundation, which can exacerbate hypersaline conditions and mangrove impact. The vegetation impacts discussed in this study are further reported on in Section 4.3 below.

4.2. Additional data

There is additional porewater data including TDS, alkalinity and ions from November 2020 to September 2021, as well as Sulfur isotope data (to investigate presence of oxidised acid sulfate soils), soil logs from 4 mangrove and 14 saltmarsh piezometers as well as soil data from vegetation quadrats. Saltmarsh invertebrate observations were also made during site inspections in affected and unaffected habitats. More recently TDS measurement from June 2022 – Sept 2022 have been collated to understand risks for any leakage of hypersaline water from the ponds and help assess if a management response should be initiated based on the trigger values established with DEW and DEM. This data is currently with the South Australia Environment Protection Authority and will be available for public review once the investigation and any possible regulatory action related to this site is completed.

4.3. Vegetation changes in the intertidal zone

The intertidal area to the west of Section 2 and 3 was aerially mapped in 1997. Nearly 1,900 ha of these habitats were mapped as being healthy, with a further 65 ha (3%) being mapped as in poor condition. This was mapped from contact aerial photography prints by hand at the time and vegetation surveys. This data provides a baseline to compare the affected vegetation post impact through 2020 and 2021 (Department for Environment and Water 2021b). There was also an observed increase in vegetation density (from aerial images) in intertidal vegetation adjacent the bund walls from 2015-2019, due to a decrease in salt scald/sediment saturation areas when the ponds level is very low or dry, however it is unclear the vegetation composition from the aerial images (i.e. the vegetation may be weedy species).

In January 2021, Department for Environment and Water (DEW) reported that 45 hectares (10 ha mangrove and 35 ha saltmarsh) of impacted vegetation at the site. Initial estimates were based on manual mapping, satellite and limited drone images.

In March 2021, the Department for Environment and Water (DEW) revised this area to 24 hectares based on new high-resolution multispectral aerial imagery over the entire salt field area and manually mapped the impacts at a fine scale (Department for Environment and Water 2021a). Given the complexities with landcover changes in intertidal zone at the temporal scale (such as tidal changes showing bare vs open water, seagrass wrack layering on saltmarsh etc) various remote sensing techniques (NDVI based delineation of vegetation condition in conjunction with ground observations and other remotely sensed analyses such as LiDAR) allowed better assessment of the extent and composition of dieback across the intertidal zone.

Key points are outlined here and expanded upon in Department for Environment and Water (2021a) and Department for Environment and Water (2021b):

- Approximately 24 hectares of vegetation dieback were mapped using new high-resolution multispectral aerial imagery captured in March 2021.
- Hyperspectral aerial imagery captured in January 2021 classified dieback mapping into types: mangrove, saltmarsh, bare ground and water.
- The new dieback boundary contains approximately 9 hectares of mangrove; 10 hectares of saltmarsh; and nearly 5 hectares of bare, sparsely vegetated, or aquatic ecosystems.
- No significant increase in the extent of vegetation death was evident between December 2020 and July 2021.
- Small areas of mangrove in poor health are detectable adjacent to the boundary of manual mapping of dead vegetation. The data shows areas of decrease in condition within approximately 50m of the boundary.
- Mangrove and coastal saltmarsh habitats in this area have shown variation in condition historically due to natural or other drivers.
- Historic 1997 mapping shows that saltmarsh adjacent to the Section 2 and 3 salt evaporation ponds showed some apparent anthropogenic impact
- March 2021 data shows some patches of saltmarsh mapped as degraded in 1997 have died (e.g., near the mangrove boardwalk), while others require further research to understand current condition.
- March 2021 data shows some patches of mangrove mapped as degraded in 1997 (e.g., south of St Kilda) declined further, while other patches (e.g., north of St Kilda) recovered.
- Further high-resolution multispectral aerial imagery will be captured along with ground observations of vegetation condition.
- All new data captured forms a high-resolution baseline for future research on these habitats.
- There is high confidence that no major areas of dead vegetation remain undetected based on the integration of new mapping and spectral analysis.

Normalised Difference Vegetation Index (NDVI) and NDVI difference mapping (dNDVI) were validated with on ground observations maps and the extent of vegetation, both alive and dead, was generated (Figure 14, Figure 15). More detail can be found in Department for Environment and Water (2021a) and Department for Environment and Water (2021b) and on the online dataviewer. It is noted that the methods used by Department for Environment and Water (2021a) did not include full spectrum hyperspectral (rather four band dataset) where species types can be distinguished. Thus, it is possible that vegetation type and positive growth identified in the imagery could be confounded, e.g. green algae blooms could be classified as living mangroves. This mapping also could not identify stressed zones, as was completed by (Dittmann et al. 2022) and discussed below.

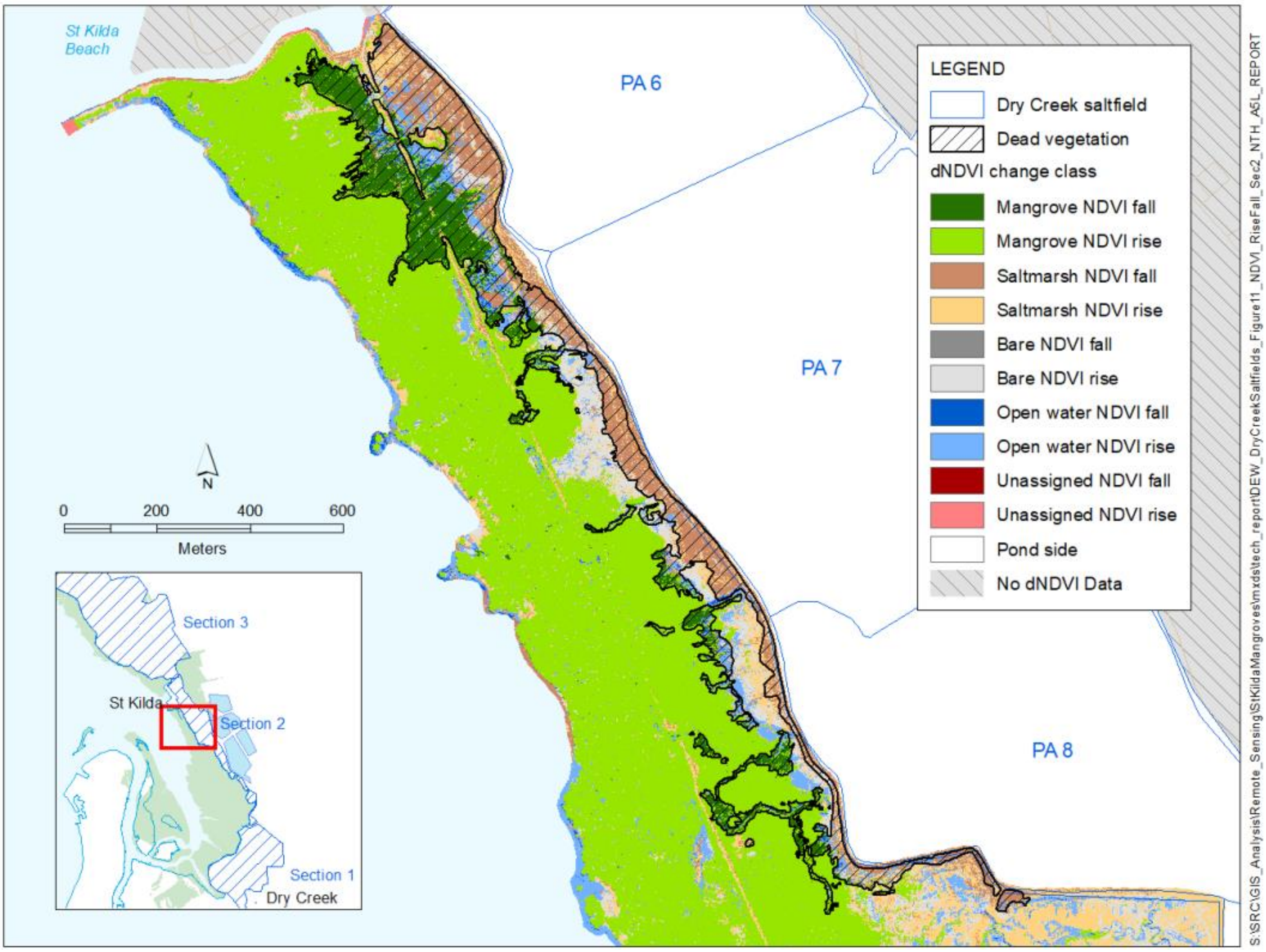

Figure 14: dNDVI thresholded hyperspectral vegetation/ land cover classes overlaid with manual mapping in northern parts of section 2 (Department for Environment and Water 2021b)

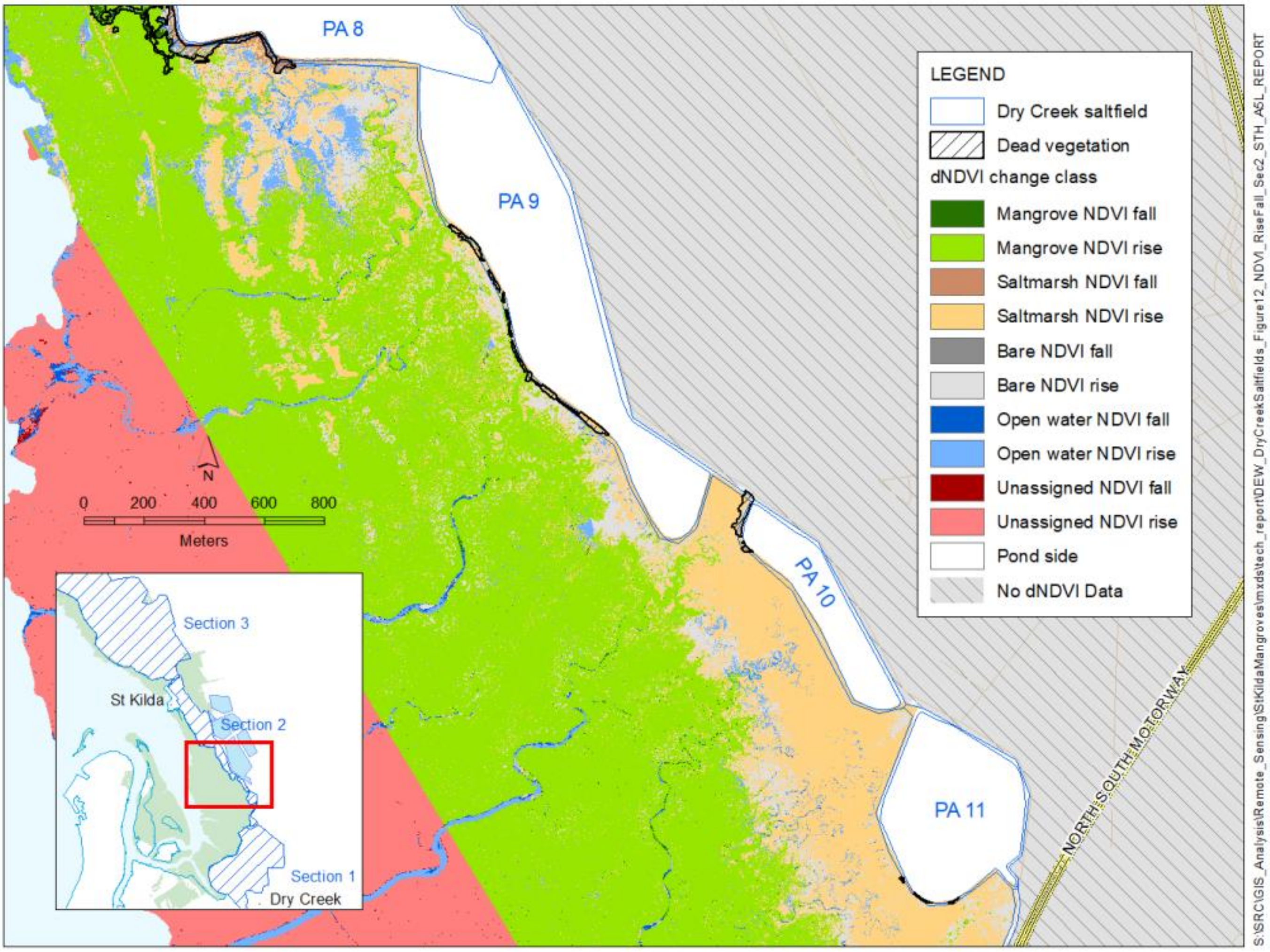

Figure 15: dNDVI thresholded hyperspectral vegetation/ land cover classes overlaid with manual mapping in southern parts of section 2 (Department for Environment and Water 2021b)

Dittmann et al. (2022) combined airborne remote sensing with on-ground proximal measurements and was able to classifies "healthy," "stressed," or "dead" mangroves from the Normalized Difference Vegetation Index – 'NDVI'. Figure 16 shows the hyperspectral imagery from (Dittmann et al. 2022) illustrating the zone of vegetation death (red) as well as the expanded stressed zone following impact (yellow). While there are vegetation areas in this region that are classified as stressed prior to impact, the mangrove stressed zone is expanded post impact.

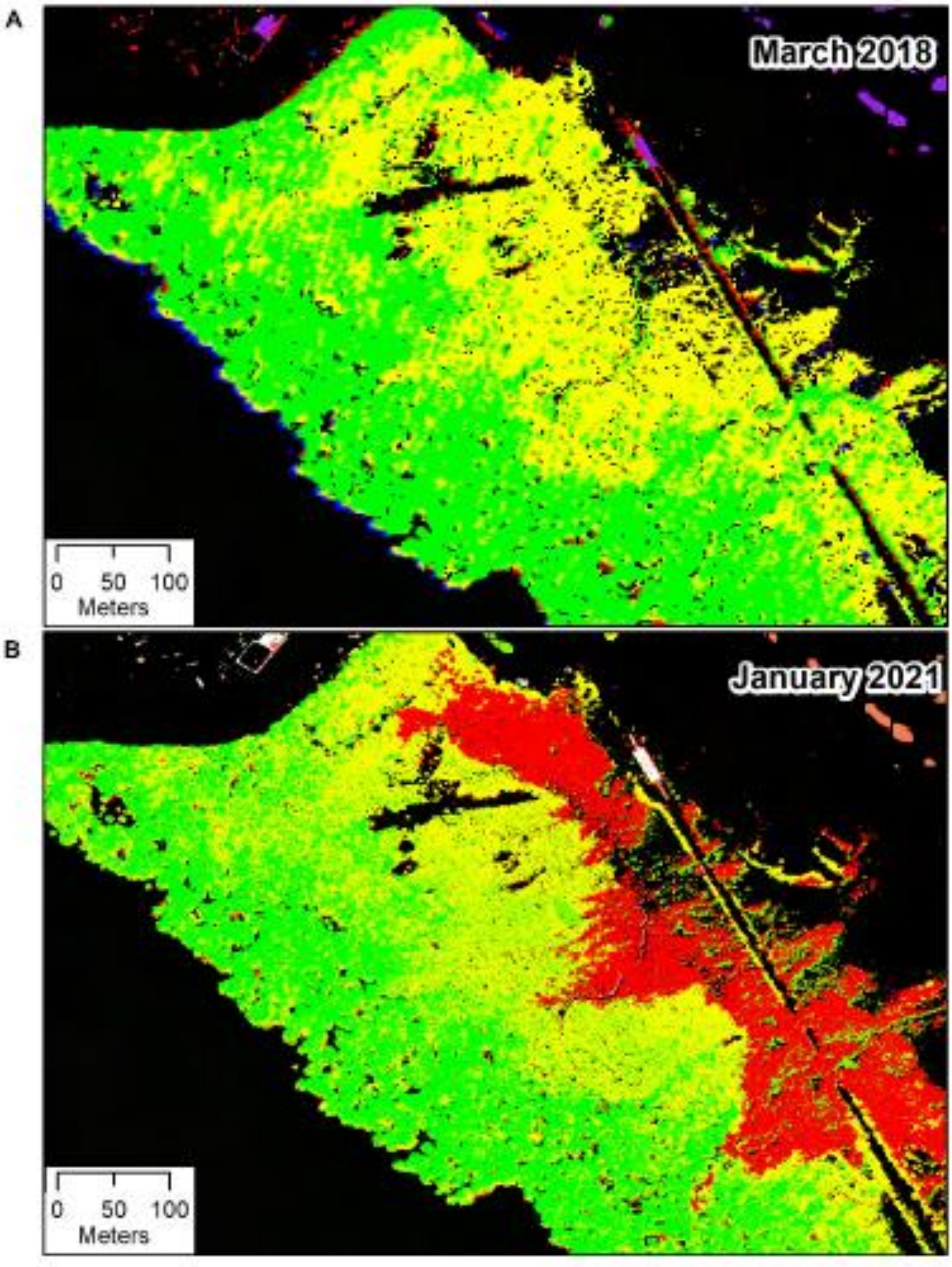

Figure 14: Hyperspectral images from the temperate mangrove forest (saltmarsh and other vegetation was masked out) near St Kilda, South Australia, from March 2018 (A) and January 2021 (B). Mangroves were classified as “healthy” (green), “stressed” (yellow), and “dead” (red). (Dittmann et al. 2022)

It is important to note that the impact area defined by (Dittmann et al. 2022) is larger than that defined by Department for Environment and Water (2021a) as this work includes both stressed vegetation areas and dead vegetation areas, whereas the work completed by Department for Environment and Water (2021a) only considers dead vegetation as the impact zone. The work completed by (Dittmann et al. 2022) demonstrates that there is likely a continuum between the current dead vegetation zone and the current healthy vegetation zone. This ‘stressed’ zone should also be considered ‘impacted’. Further analysis of the stressed vegetation zone could further define the impact vegetation area, and mapping over temporal scale would allow further analysis of any recovery in condition. Finer level hyperspectral analysis could potentially define areas down to species level, which would be useful to prevent inaccuracies between vegetation classification using NDVI and dNDVI and could potentially highlight a greater impacted area than the hyperspectral work completed by Department for Environment and Water (2021a).

Six saltmarsh transects and quadrats were surveyed in March and April 2021 and then resurveyed in October/November 2021 (Fotheringham and Detmar 2021). Three transects were affected by vegetation death and three transects were unimpacted in sampling in March/April. Results are summarised here and are explained (with vegetation type and cover descriptions) in Fotheringham and Detmar (2021).

Transect 1 (148 m) recorded severe dieback in the initial survey but this had not increased in the resurvey. Regeneration of vegetation of some species that had been affected but not killed was observed. Transect 2 (116 m) was severely affected by dieback with 98% -100% of vegetation killed. The site was covered by green algae in the resurvey. There was also a decrease in vegetation cover, either by decomposition or physical removal. A *Suaeda australis* seedling was recorded in quadrat 1 and seedlings (*Salicornia quinqueflora* and *Suaeda australis*) were sparsely present. Transect 3 (43m) was severely affected by vegetation death (98%) with vegetation in the resurvey also dead to the same extent (*Tecticornia arbuscula* low open shrubland).

Transect 4, 5 and 6 were unaffected by vegetation death and still unaffected in the resurvey

Overall, the report concluded:

- The vegetation death does not appear to have expanded in the affected transect sites between surveys. The three transects that were healthy in April remained healthy in November.
- Some saltmarsh plants affected but not killed by the in some locations along the first three transects appear to be still surviving.
- Seedlings of mainly *Salicornia quinqueflora* but also *Suaeda australis* are appearing in the upper parts of impacted saltmarsh. Seedling were not observed in the lower parts of the saltmarsh towards the mangrove edge.
- There has been loss of affected plants in impacted areas. Saltmarsh communities on low marsh sites appear to have decomposed faster than more elevated communities.

It is important to note that to date a vegetation resurvey has not been completed during 2022, and therefore any trend of vegetation recovery needs to be supported with ongoing data seasonal and yearly data. In addition, species type, density, community composition and propagule size are important distinctions when new growth is recorded in vegetation in the surveyed transects, especially those where vegetation death was extensive. The simple presence of seedlings may not in itself be a sign of sediment recovery, given that some species are opportunistic, and others such as mangroves propagules can take some months to lay down root systems into sediments. Whole of ecosystem recovery should be quantified to illustrate the system recovery, rather than individual species emergence.

4.4. Barriers to tidal flushing and associated vegetation impacts

It is clear from the pattern of vegetation death in the intertidal zone, that certain areas in the intertidal zone are more affected than others. Vegetation death typically runs along creek lines, through breaches in the boardwalk bund and in the area just adjacent the bund walls (typically scour areas when bund wall material was collected). These areas are typically lower elevation areas in the landscape. Initially, when the hydraulic gradient from the pond to the intertidal zone was higher, these lower elevation areas would have been the typical flow pathways for hypersaline brine in the intertidal zone. Vegetation death would have occurred as brine discharged into these areas and flowed through and accumulated in the vegetation root zone. Hypersaline brine may have then accumulated and remained at depth, due to tidal flushing diluting surficial sediments only.

In the northern section of the intertidal zone vegetation is severely affected on either side of the boardwalk bund wall (scour areas) and shows a wider lateral pattern of vegetation death compared to the southern sections. In the northern section, there are several barriers to tidal flow. These include the marina bund wall to the north and chenier (old sand dunes) ridges to the west. These barriers would have limited the amount of seawater movement in the adjacent areas with each tidal cycle. Without good tidal exchange salt would have been able to accumulate in the landscape and spread laterally. In addition, the only breach of the boardwalk bund in this northern section, is around 350 m to the south of the Marina, allowing tidal flushing in one end only between the boardwalk bund and the Section 2 bund. This would not have received the extent of tidal flushing than an area which has an inlet and outlet for the tidal flow, such as those areas further south. Similarly, the area west of the boardwalk bund and just south of the Marina would have limited tidal flushing due to higher elevation chenier ridges to the west. Increased tidal flow through the boardwalk bund to the north near the marina may increase the extent of tidal flow available to this area. The barriers to tidal flushing are represented and visually presented in the conceptual site model (CSM).

The pattern of vegetation death along tidal creeks which adjoin remnant creek lines inside the pond is also noted. This is likely due to the pathway of hypersaline water through the groundwater under the pond along these old creek lines, into existing creek lines in the intertidal zone.

5. Knowledge gaps and data limitations

The conceptual model improves our understanding of processes in the pond and the adjacent intertidal zone. The data underlying this model suggests that the impact to the intertidal zone was a result of leakage of extremely hypersaline water from the ponds of Section 2 when they were refilled from December 2019 to October 2020. The data also suggests that there is recovery of some sediments to pre-impact salinities in some areas (EPA data) and emergence of some seedlings in areas which did not suffer complete vegetation death (Fotheringham and Detmar 2021). However, more data is required to quantify trends towards sediment and vegetation recovery.

The intertidal sediments adjacent Section 2 are particularly heterogenous as a result of the changes to the landscape from the construction of the salt evaporation ponds, and subsequent sediment/vegetation processes which developed in the area as a result. The level of heterogeneity in the intertidal sediments makes broad scale assumptions about the recovery from the hypersaline water in the intertidal zone difficult. Higher resolution data could further refine intertidal soil/sediment type, aquifer boundaries, salt flux, bund wall permeability and aquifer confining layers.

It is highly likely that salt accumulation and flushing are spatially variable, with very localised changes occurring both horizontally (across the landscape – within meters) and vertically (down the profile – within centimetres). There are most likely areas of hydraulic flow from the hypersaline ponds in Section 2 to certain areas in the intertidal zone, while other areas may remain unaffected. For example, remnant creek lines from the pond and under the bund may represent a hydraulic pathway for hypersaline water while barriers to tidal flushing (boardwalk bund, old chenier ridges, semi permeable sediment layers, scour areas etc) limit tidal flushing across some areas and at depth within a soil profile.

Changes in salinity also occur in this landscape temporally, with daily (tides/ precipitation) and seasonal changes (summer evaporation/winter ponding). Larger storms/tides in winter increase tidal flushing in the intertidal zone but also increase hydraulic heads in the pond with resulting surface water ponding. Summer periods increase evaporation in the pond (decrease hydraulic head to the intertidal zone) but can also evaporate the hypersaline salts still accumulated in the intertidal zone.

There has been no on ground monitoring of vegetation transects or soil pore waters has been conducted in 2022 which prevents any quantitative assessment of trends in recovery impossible. The lack of widescale spatial and temporal whole of ecosystem assessments (i.e. benthic invertebrates) across the sites also does not allow potential recovery trends to be assessed. It is also noted that some areas are incredibly difficult to access in this zone (finer, muddier sediments do not allow access for sampling or piezometer installation) so data may, in some cases, represent only areas which allow access to sediment/groundwater sampling.

An integrated monitoring program is recommended to be designed and implemented to assess the response of the saltmarsh and mangrove ecosystem in affected and unaffected parts of the intertidal zone. A better understanding the tidal water movement pathways across the site, both at present and predicted into the future, would also allow a better assessment of barriers to tidal flushing, which could inform recovery pathways.

6. References

BDC 2020. Dry Creek Salt Field - Integrated Program for Environment Protection and Rehabilitation and Mine Operations Plan - Revision 4 v.1. In*:* LTD, BDCP (Ed.).

BELPERIO AP, MURRAY-WALLACE CV AND CANN JH. 1995. The last interglacial shoreline in southern Australia: Morphostratigraphic variations in a temperate carbonate setting. Quaternary International 26: 7-19.

COLEMAN P, COLEMAN F AND FOTHERINGHAM D 2017. Thornbills, samphires & saltmarsh tipping points: A assessment of potential threats to Samphire Thornbill habitat

in the northern Adelaide & Mt Lofty Ranges Natural Resources Management region Delta Environmental Consulting.

DEPARTMENT FOR ENVIRONMENT AND WATER 2021a. Dry Creek salt fields vegetation impact mapping - Technical Report. DEW Technical report 2021/14.

DEPARTMENT FOR ENVIRONMENT AND WATER 2021b. Dry Creek salt fields vegetation impact mapping Summary report. Government of South Australia.

DEW 2021. Dry Creek salt fields vegetation impact mapping Summary report. Summary report of DEW Technical report 2021/14: Government of South Australian Department for Environment & Water.

DITTMANN S, MOSLEY L, STANGOULIS J, NGUYEN VL, BEAUMONT K, DANG T, GUAN H, GUTIERREZ-JURADO K, LAM-GORDILLO O AND MCGRATH A. 2022. Effects of Extreme Salinity Stress on a Temperate Mangrove Ecosystem. Frontiers in Forests and Global Change 5.

FITZPATRICK RW, SHAND P, BAKER AKM, GROCKE S AND THOMAS BT 2014. Dry Creek Salt Fields: Assessment of Acid Sulfate Soil environments in Section 2 for ponds (PA3 to PA12) and drains. Acid Sulfate Soils Report No ASSC_067, The University of Adelaide: The University of Adelaide.

FOTHERINGHAM D, DETMAR SA, TURNER A, LY K, RITCHIE R AND BESWIC F 2019. Observations concerning a monitored saltmarsh at Pt Pirie, Spencer Gulf, South Australia. Coast and Marine Branch

Department for Environment and Water (DEW), South Australia.

FOTHERINGHAM DG AND DETMAR SA 2021. Re-survey of six saltmarsh transects near St Kilda

October/November 2021. Report prepared for the Environment Protection Authority.

LIONBERGER ML, SCHOELLHAMER DH, BUCHANAN PA AND MEYER S 2004. Salt-Pond Box Model (SPOOM) and Its Application to the Napa-Sonoma Salt Ponds, San Francisco Bay, California. In*:* SURVEY, USG (Ed.) US Geological Survey Water Resources Investigations Report 03-4199, , California, p. 21.

LOVELOCK CE, FELLER IC, REEF R, HICKEY S AND BALL MC. 2017. Mangrove dieback during fluctuating sea levels. Scientific Reports 7: 1680.

MOSLEY L 2014. Geochemical modelling of the likelihood of gypsum precipitation or dissolution following discharge of saline water to a trial pond near Bolivar. Water Quality Science.

SA WATER 2016. Monitoring and Management Plan Dry Creek Salt Field Recycled Water Trial. Environmental Opportunities Team, Strategy and Planning Division, SA Water.

SAVE ST KILDA MANGROVES ALLIANCE 2021. Managing the Holding Pattern to the north of St Kilda, SA.

THOMAS BP. 2010. Coastal acid sulfate soil processes in Barker Inlet, South Australia. The University of Adelaide.

TONKIN 2015. Dry Creek Salt Fields: Shallow Piezometers Installation and Monitoring. Tonkin Consulting.

WOOD L. 2022. Assessing impacts of hypersalinity on a coastal saltmarsh community in South Australia. Honours, The University of Adelaide.

7. Acknowledgements

We thank the Department for Environment and Water (DEW) for their input and guidance, in particular Sandy Carruthers, Dan Rogers, Matthew Miles and Doug Fotheringham. We also thank Gabor Bekesi from the Department for Energy and Mining (DEM), and David Palmer and Peter Goonan from the South Australian Environment Protection Authority for their valuable data and input.

We kindly thank Peri Coleman from Delta Environment Consulting and Faith Coleman from EcoProTem Consulting for sharing their local knowledge of the saltfield and coastal ecosystems.

We also kindly thank Dr. Alice Jones from the University of Adelaide and Prof. Sabine Dittmann from Flinders University.

8. APPENDIX 1

Transect A Salt Index, Dry Creek Saltfields

Gabor Bekesi, Principal Hydrogeologist, Department for Energy and Mining, 4 October 2022

Summary

The Transect A salt index was developed to track temporal changes in the salt flow (or salt flux) from beneath the western saltpond PA6 towards the salt marsh. The index is calculated from groundwater head measurements at seven sites, and salinity from one well. Groundwater heads are corrected to density and the influence of viscosity is incorporated into the Transect A salt index, based on Dead Sea research involving salinities similar to those measured adjacent to the salt ponds. By relating salt flux to that in November 2020 (the "*index*" concept), the influence of a key and unknown parameter, the hydraulic conductivity, can be minimised

The Transect A salt index is based on several assumptions, and it represents a simplified single quantitative measure of the complex trends in salt flux near Transect A.

The Transect A salt index is entirely based on existing measurements and is not a predictive (model) tool. Notwithstanding, there are seasonal and longer-term trends in Transect A salt index that are discussed and interpreted.

Background

Hypersaline groundwater from beneath a salt pond (PA6) flows towards the salt marsh and transports salt that had caused an impact on the vegetation of the salt marsh.

SA government has monitored groundwater at the Dry Creek saltfields since late 2020. There are up to 50 sites monitored along what is known as '*Section 2*" (saltponds PA6-PA11, Figure 1), including those along transect A. Transect A is the closest transect to the impacted vegetation (mostly mangroves) area that covers the entire width of a salt pond (PA6), from east to west and into the salt marsh.

Objectives

The objective of this report is to document the purpose, principles, and calculations of the Transect A salt index.

The Transect A salt index was developed to measure or track the temporal changes in the salt flux, from beneath the western saltpond PA6, towards the salt marsh.

Figure 1. Groundwater Monitoring transects and salt ponds at St Kilda

Salt flux

Salt flux (**S**), across a 1 m long section perpendicular to the groundwater flow, at a time **t,** can be calculated as the product of groundwater flow (**q**) and salt concentration in the groundwater (**C**):

$$S = q(t)\ C(t) \qquad (1)$$

The simplest applicable formula for calculating groundwater flow across a 1 m long section perpendicular to the flow (**q**), from beneath the ponds towards the salt marsh is derived from the Darcy Equation for an unconfined aquifer by Ritzema (2006; the formula is identical to the “Dupuit Equation” often used to describe unconfined groundwater flow) for a vertical dam:

$$q = k\ (H_1(t)^2 - H_2(t)^2)\ /\ 2L \qquad (2)$$

k is the hydraulic conductivity for the aquifer, m/d

H_1 is the groundwater head beneath the western salt ponds, above the base of the aquifer, m

H_2 is the groundwater head in the salt marsh above the base of the aquifer, m. The base of the aquifer, along the western side of Transect A, is set at -1 m AHD, based on the drill log of P01 (Tonkin Consulting, 2015)

L is the lateral distance between the measurement points for H_1 and H_2, m

(t) denotes that preceding parameter is time dependent

Substituting Equation 2 into 1:

$$S = k\, C(t)\, (H_1(t)^2 - H_2(t)^2) / 2L \qquad (3)$$

Permeability, hydraulic conductivity, and viscosity

Viscosity is the resistance of a fluid to flow. In most natural aquatic environments, the salinity is relatively low, and changes in viscosity are minor and typically considered to be negligible. In hypersaline environments, this simplification is not justified since viscosity and density vary significantly and are thus expected to be important factors controlling groundwater flow (Weisbrod et al., 2016).

Viscous fluids, including brines, flow slower than pure water. This is recognised by the relationship between hydraulic conductivity (property of both medium and fluid) and permeability (property of media only) that includes both density and dynamic viscosity as variables:

$$k = K(t)\, \rho(t, \mu)\, g / \mu(t) \qquad (4)$$

where

- K is the permeability, m^2
- μ is the dynamic viscosity of the fluid, Pa s or kg/(m s)
- ρ is the density of the fluid, kg/m^3
- g is the acceleration due to gravity, m/s^2.

The relationship between density and viscosity

In especially the northern, arid part of SA, there are known hypersaline aquifers with salinities up to three times that of seawater. As Figures A1 and A2 of Appendix A illustrate, the increase in viscosity due to increased density/salinity at those salinities is limited. As a result, and to the writer's knowledge, to date there has not been a need for research on the relationship between groundwater viscosity and density in SA.

Groundwater beneath pond PA6, however, has been up to nine times the salinity of seawater and represented a significant increase in viscosity and therefore a challenge on a new scale. A relationship from Dead Sea research (personal comm., T Collaton, EPA, 2021; Karcz and Zak, 1987, and Weisbrod et al., 2016), that has salinities similar to groundwater beneath the salt ponds, was developed.

Overall, based on the Dead Sea research, for Dry Creek NaCl brine solutions, a reduction of hydraulic conductivity to about 50% of that of pure water may be expected (from Appendix A) at a specific gravity of 1.2 to 1.25 (corresponding to 300,000 to 360,000 mg/L TDS). That is, the hypersaline groundwater beneath the ponds will flow with about half the velocity of pure water, assuming 20ºC temperature. Higher temperature would increase hydraulic conductivity and groundwater flow. Although there is limited knowledge of the changes in ion concentration in the brine, given the high level of TDS, it is likely the brine is dominated by halite (NaCl). Higher magnesium content would decrease the hydraulic conductivity (and decrease the groundwater flow).

Salt flux adjusted to density and viscosity

Substituting Equation 4 to 3:

$$S = K(t)\ \rho(t)\ g\ C(t)\ (H_1(t)^2 - H_2(t)^2)\ /\ (2L\ \mu(\rho,t)) \quad (5)$$

In Equation 5, the inputs can be classified as follows:

- **g** and **L** are known constants
- **ρ**(t) and **C**(t) can be independently measured. If, however, one of **ρ** or **C** is known, at the salinities involved, the other parameter can reliably be estimated
- $\mathbf{H_1}$(t) and $\mathbf{H_2}$(t) can be measured, and subsequently calculated from the measurement and data from Tonkin Consulting (2015)
- **μ**(t) can be estimated from **ρ**(t) based on Dead Sea research (Karcz and Zak, 1987; and Weisbrod et al., 2016, refer to Appendix A)**.**
- the permeability (**K**) is unknown; although could be estimated probably within an order of magnitude.

To overcome the unknown **K**, a salt index, relative to November 2020, was developed:

$$S_{index} = S(t)\ /S_{Nov.2020} \quad (6)$$

By relating the salt flux at a time (t) to that in November 2020, **K**, **g**, and **L** are eliminated from Equation 6 and all the remaining input variables can be measured or assessed.

The calculation of the Transect A salt flux index

The Transect A salt flux index is calculated from measured/estimated data from up to eight wells as follows:

- Density corrected groundwater head measurements (H_1 and H_2) above the base of the aquifer are calculated from up to seven wells:

  $(H_1(t)^2 - H_2(t)^2 = H_{ave}^2(t, P02,P03,P04,P05) – H_{ave}^2(t, SK8, SK9,SK10)$
  Using average heads is to minimise the risk to a single erroneous or missing measurement.

- Salinity (measured as Total Dissolved Solids or TDS) is from well P01 (Figure 2). P01 is the bund well, between PA6 (from beneath the groundwater flows) and the salt marsh (where the groundwater flows into).

  C = C(t, P01) C is obtained either from laboratory results (as TDS) or calculated from density (hydrometer) measurements.

- ρ/μ is estimated from Karcz and Zak, 1987 and Weisbrod et al., 2016.

The calculation method for the Transect A salt index was improved in May 2022. The calculation of groundwater flow now includes the variations in the saturated aquifer thickness and the terminology has also changed from '*hydraulic gradient*' to '*head differences*'. When groundwater heads increase, so does the average saturated aquifer thickness through which groundwater flow occurs. Aquifer homogeneity is still an assumption, that is the hydraulic conductivity of the aquifer is the same everywhere.

The trends described under the heading 'Discussion and analysis', however, did not change. The average change in the calculated Transect A salt index is -2% (the improved index is smaller, In average by 2%) and the absolute changes are all between -6% and +3%.

Figure 2. Close up of Transect A (solid line) at the western side of PA6

Discussion and analysis

The Transect A salt index curve (black curve in Figure 3) is a measure of trends in the salt moving west from beneath the salt ponds towards the salt marsh: a product of the hydraulic head difference (blue curve in Figure 3, between groundwater under the pond and groundwater under the marsh), and the salinity (brown curve in Figure 3, adjusted for viscosity (resistance against flow due to the amount of salt).

The Transect A salt index is entirely based on existing measurements and is not a predictive (model) tool. Notwithstanding, there are seasonal and longer-term trends in Transect A salt index that are discussed and interpreted below:

- November 2020 to June 2021: a steep decline occurred due to the cessation of brine transfer to Pond PA6 (Environmental Direction), the summer (lack of rainfall and high evaporation), and EPA water transfers in March/April 2021.

  The decline in the Transect A salt index, from 100% to 40%, during this period is driven by a decline in the hydraulic head difference.

- June to November 2021: increasing head difference (winter rain recharge) was offset by a significant reduction in salinity (almost certainly the result of tidal influence.

  The Transect A salt index remained stable around 40%, driven by an increase in hydraulic head difference and a significant decrease in salinity. The two processes cancelled each other maintaining the index at 40%.

- November 2021 to April 2022: The Transect A salt index decreased due to decreasing head difference (summer lack of rainfall and high evaporation) and stable salinity. The decline in the Transect A salt index, from 40% to 25%, during this period is driven by a decline in the hydraulic head difference. Notwithstanding this trend, there is still considerable salt load present under PA6.

Groundwater head (Figure 4):

- Groundwater heads beneath and to the east of PA6 show trends similar to the Transect A salt index, a long-term decline super-positioned to a seasonal variation (high heads in winter and low in summer). Beneath the bund (P01, orange curve) and below the salt marsh (green curves) the groundwater heads are gently declining with small seasonal variations, consistent with the proximity of large amounts of surface water controlling/limiting groundwater variations.

Groundwater salinity (Figure 5):

- Salinity in the pond PA6 (thick brown curve) is very high and forms a maximum limit to groundwater; a strong indication that the pond is the source of groundwater salinity.
- Groundwater salinity was stable below the eastern pond (black, purple and blue curves) and shows a small increase to June 2021 beneath the western PA6 (red curves) followed by a small decline to September 2021.
- Groundwater salinity in P01 (orange curve) indicates a significant reduction between February and September 2021, almost certainly the result of tidal influence.
- Groundwater salinity below the salt marsh is gently declining with a steep reduction between March and June 2021.

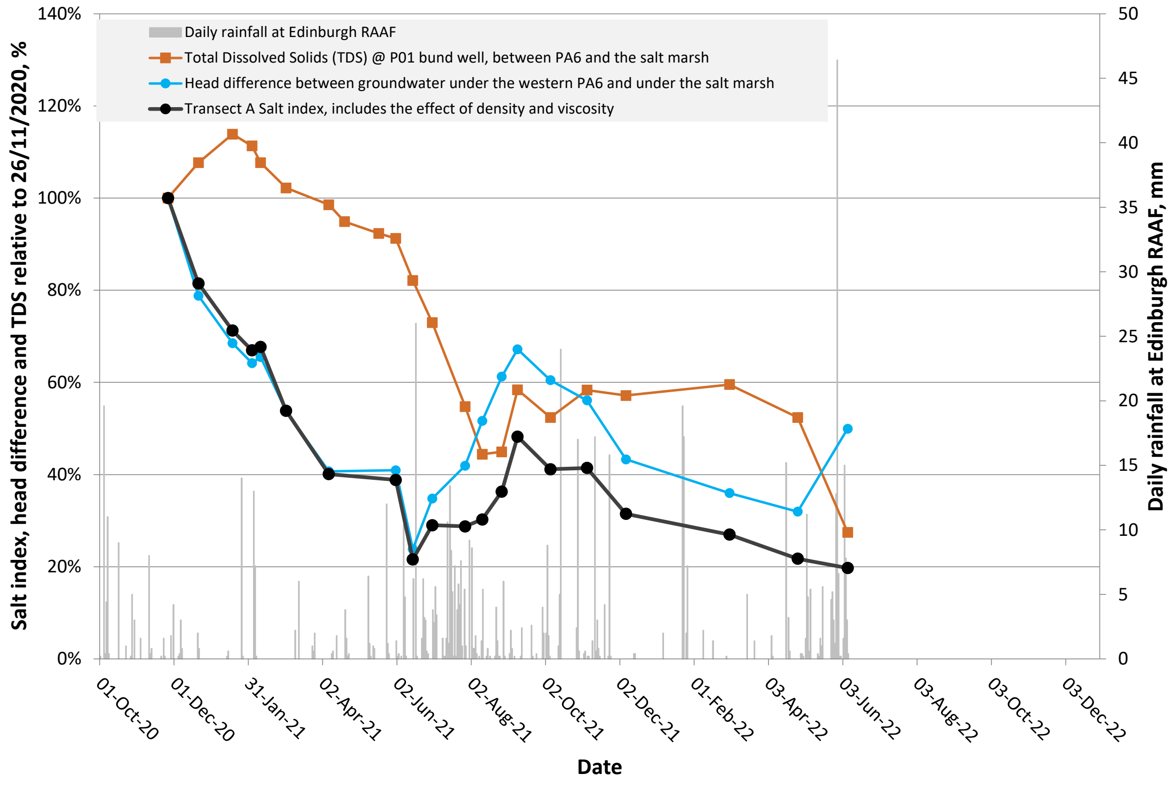

Figure 3. Transect A salt index

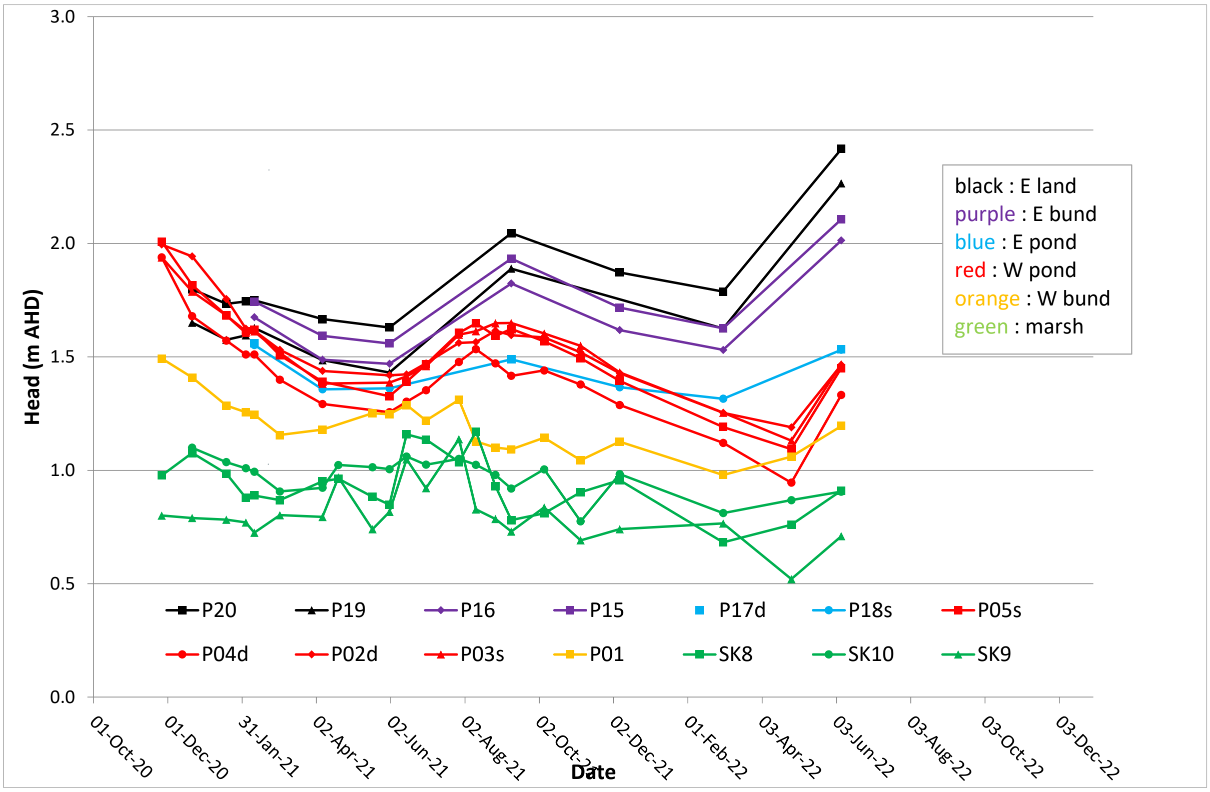

Figure 4. Transect A - groundwater heads

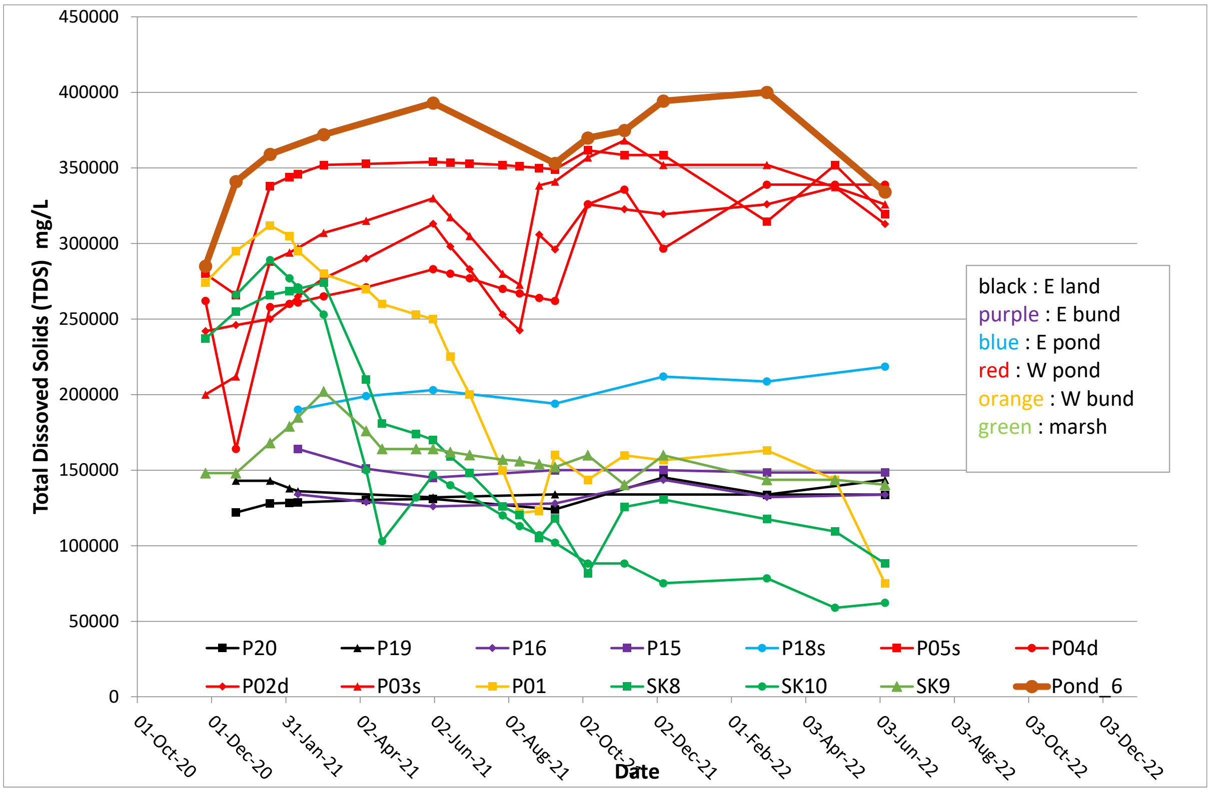

Figure 5. Transect A - groundwater salinity (Total Dissolved Solids or TDS)

Assumptions and simplifications

It is important to note that the Transect A salt index is a simple measure of complex processes and is based on several simplifications and assumptions:

- Groundwater flow is assumed to occur as a result of a hydraulic gradient. In reality there is also a density contrast, between the groundwater beneath PA6 and groundwater below the marsh, that can drive purely density driven (convective) groundwater and salt flow; such convective flow is neglected for the purposes of the Transect A salt index.
- The Transect A Salt Index is based on data from one transect only. Additional transects and data would allow further information of the percentage changes in salt flux; however, the current well configuration does not allow for that.
- The Tonkin Consulting (2015) and EPA wells below the salt marsh represent the salinity of the entire aquifer. In reality, discretisation with depth would occur.
- The hydraulic conductivity of the aquifer is homogeneous. In reality, the aquifer may be inhomogeneous.
- The salinity in P01, measured earlier as laboratory TDS (total dissolved solids) and lately from in-situ groundwater density measurements, represents the salinity of groundwater between the western P06 and the marsh. In reality, there may be variations in salinity. Tonkin Consulting (2015) and data collected since November 2020 illustrate that groundwater under the bund and in some western pond wells are influenced by the tidal cycle (under the leaky bund). The impact of the tide on the transfer of salt from below the western pond PA6 to the adjoining saltmarsh, based on a single salinity measurement from the single well P01 could potentially skew the saltindex.
- Wells P01 to P05, and SK8 to SK10 form a line parallel to groundwater flow. In reality, some wells are offset from the straight line of Transect A (Figure 2).

Acknowledgements

The great help provided by Taryn Collaton of the EPA by identifying and obtaining the Dead Sea research papers (Karcz and Zak, 1987 and Weisbrod et al., 2016) and the constructive review comments of Emily Leyden of the University of Adelaide are gratefully acknowledged.

References

Karcz, I., and I. Zak, (1987). Bedforms in salt deposits of the Dead Sea brines: Journal of Sedimentary Petrology, v. 57, p. 723-735.

Ritzema H P (editor in-chief) (2006). Drainage Principles and Applications. Wageningen, Alterra, ILRI Publication No.16.

Tonkin Consulting (2015). Dry Creek Salt Fields Shallow Piezometers Installation and Monitoring

SA WATER, 18 December 2014. Ref No. 20141458R01.

Weisbrod N, Yechieli, Y, Shandalov, S, Lensky, N (2016). On the viscosity of natural hyper-saline solutions and its importance: The Dead Sea brines. Journal of Hydrology 532 (2016) 46–51.

Appendix A.

Selected aspects of Dead Sea research

Karcz and Zak (1987):

- The average salinity of seawater is 35,000 mg/L with a density of 1030 kg/m^3.
- The dynamic viscosity of pure water is 1 cp (1 centi Poise or 1 cp=10^{-3} Pa s)
- NaCl brines reach about 2 cp at a specific gravity of 1.2.
- $MgCl_2$ brines reach about 4 cp at a specific gravity of 1.21.

The chemical composition significantly affects the dynamic viscosity of brines with similar densities. Solutions with a higher Mg/Na ratio have higher viscosity (Weisbrod et al. 2016). The dynamic viscosity is also dependent on temperature.

Weisbrod et al. (2016) suggest that the dynamic viscosity of Dead Sea brines (specific gravity ~ 1.24) varies between 2 and just above 3 cP at temperatures of 20-30 ºC. Further analysis of diluted samples of Dead Sea brines suggests that a change of the specific gravity from 1.15 to 1.24 increases the dynamic viscosity from about 2 cP to 3.2 cP at 20 ºC (Weisbrod et al., 2016).

The combined effects of dynamic viscosity and density for Dead Sea brines (specific gravity of 1.24) and for the more extremely saline natural brine (specific gravity of 1.37) were found to be a reduction of hydraulic conductivity to between about 15% and 30% of that of pure water (Weisbrod et al. 2016). Figures A1 and A2 of Weisbrod et al. (2016) suggests a reduction of hydraulic conductivity to about 35% for Dead Sea brines (DSB) and to about 60% for NaCl brines at ρ =1.2 kg/m^3 and 20 ºC. These reductions are calculated from pure water.

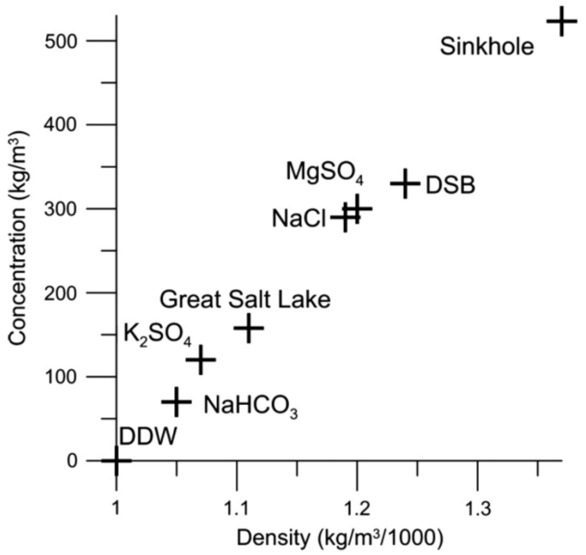

Figure A1 Density vs. total salt concentrations of the natural and artificial brines after Weisbrod et al. (2016). DDW=double-distilled water; DSB=Dead Sea Brines.

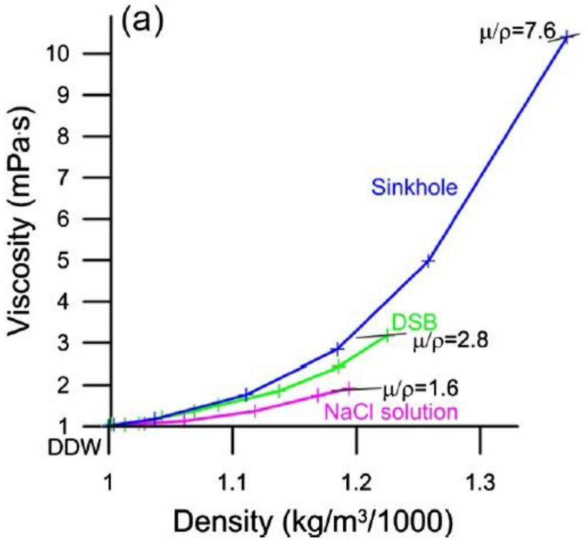

Figure A2. Dynamic viscosity (μ) vs. density (ρ) of various solutions at 20 ºC after Weisbrod et al. (2016), DDW=double-distilled water; DSB=Dead Sea Brines.

Using the values from Karcz and Zak (1987) suggest a reduction of hydraulic conductivity to about 60% of that of pure water for NaCl brines at ρ =1.2 kg/m^3 ; and to 30% of that of pure water for $MgCl_2$ brines at ρ =1.22 kg/m^3 at 20 ºC. These results are consistent with the higher end (NaCl solutions) of Weisbrod et al. (2016).

Overall, for Dry Creek NaCl brine solutions a reduction of hydraulic conductivity to about 50% of that of pure water may be expected at a specific gravity of 1.2 (corresponding to 250,000 to 300,000 mg/L TDS). That is, the hypersaline groundwater beneath the ponds will flow with about half the velocity of pure water, assuming 20ºC temperature. Higher temperature would increase hydraulic conductivity and higher Mg content would decrease the hydraulic conductivity (and groundwater flow).